Table 4: Distribution of water-bearing zones in Madison strata penetrated by well.

Depth Interval (feet)	Thickness (feet)	Relative Porosity
2385 - 2433	48	High
2445 - 2451	6	High
2456 - 2522	66	High
2538 - 2544	6	High
2560 - 2606	46	High
2621 - 2644	23	High
2648 - 2656	8	High
2668 - 2704	36	High
2710 - 2720	10	High
2728 - 2752	24	High
	273	

The total thickness of Madison strata identified from a depth of 2370 to 2752 feet is 382 feet. The zones of relatively high porosity identified from the resistivity logs and summarized on Table 4 are interpreted to be the principal water-bearing zones in the Madison strata penetrated by this well and total 273 feet or 71.5 percent of the thickness of Madison strata penetrated. The distribution of the zones of high resistivity shown on Figure 21, which are interpreted to be the principal water-bearing zones in the Madison aquifer at this well, underscore the importance of fully penetrating the entire aquifer with the well to optimize well yield.

5 YIELD AND DRAWDOWN TESTS

Test Well #2A was initially tested in mid-October 2012. The static water level and barometric pressure were monitored from 10/13/2012 through 10/16/2012 prior to starting a stepped rate pumping test on 10/18/2012, after installation of a test pump on 10/16/2012 and 10/17/2012. The step test was terminated due to excessive vibration in the test pump, after one 510-gpm step of 181-minutes duration and 152 minutes at 650 gpm. The results of the brief step test indicated that the well performance was considerably less than required, and the well was stimulated with a high-pressure acid treatment described in the previous section of this report. After acid stimulation, the well was subjected to a second stepped rate test followed by a 48-hour constant rate test at 1500 gpm. The 1500-gpm constant rate test was limited by the capacity of the available test pump, not the well yield; however, it exceeded the design specifications for a 1400-gpm well.

5.1 Pre-Test Monitoring

Figure 22 shows the pre-test monitoring static water level and atmospheric pressure. It is evident that as the barometric pressure decreases, the static water level in the

aquifer, as observed in Test Well #2A, declines. This response is the classic relationship of an increase in atmospheric pressure imposing more load on the land surface, increasing the grain-to-grain load on the mineral matrix of the aquifer; thus compressing the pores in the aquifer with a resultant rise in groundwater levels (pore pressure) in the aquifer. On Figure 22, a decrease in atmospheric pressure corresponds to a reduction in the load on the aquifer, relaxation of compression of aquifer pores, and a resultant decline in the static water level (pore pressure).

Figure 22: Pre-test monitoring static water level and barometric pressure.

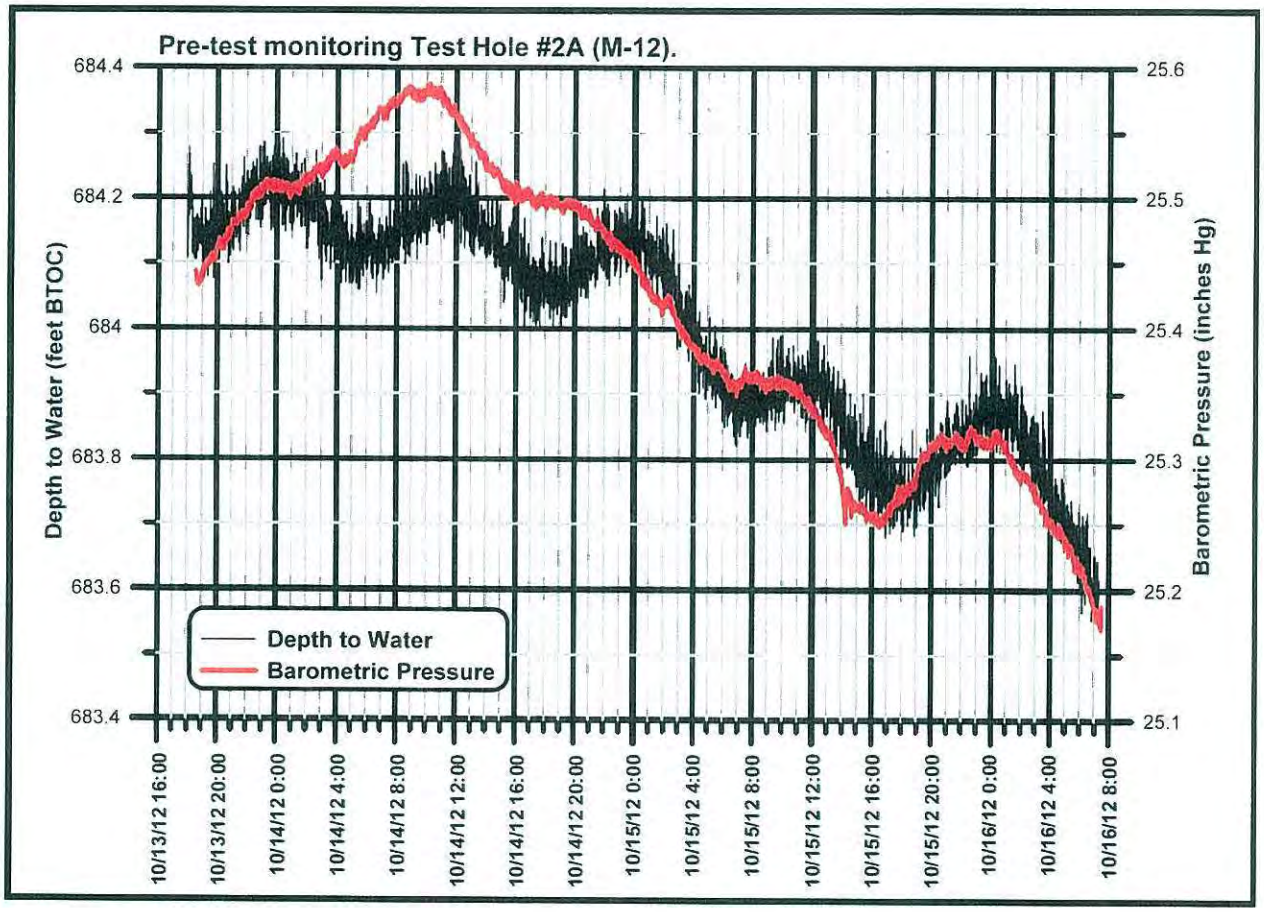

The relationship between barometric pressure change and static water level fluctuation is shown on Figure 23. The data plot reflects the fact that when barometric pressure is relatively constant or fluctuating within a relatively narrow range, there is little fluctuation in the groundwater level. This is evident as a "cloud" of data on the right-hand side of the plot on Figure 23, where the data correspond to the 6:00 p.m., 10/13/2012 through 4:00 p.m., 10/14/2012 plot on Figure 22. The remainder of the data correspond to the part of Figure 22 after 4:00 p.m., 10/14/2012, and describe a strong relationship between the barometric pressure change and a corresponding and resulting change in the static water level in the aquifer, through which a linear regression line is shown on Figure 23.

Figure 23: Change in static water level versus change in barometric pressure.

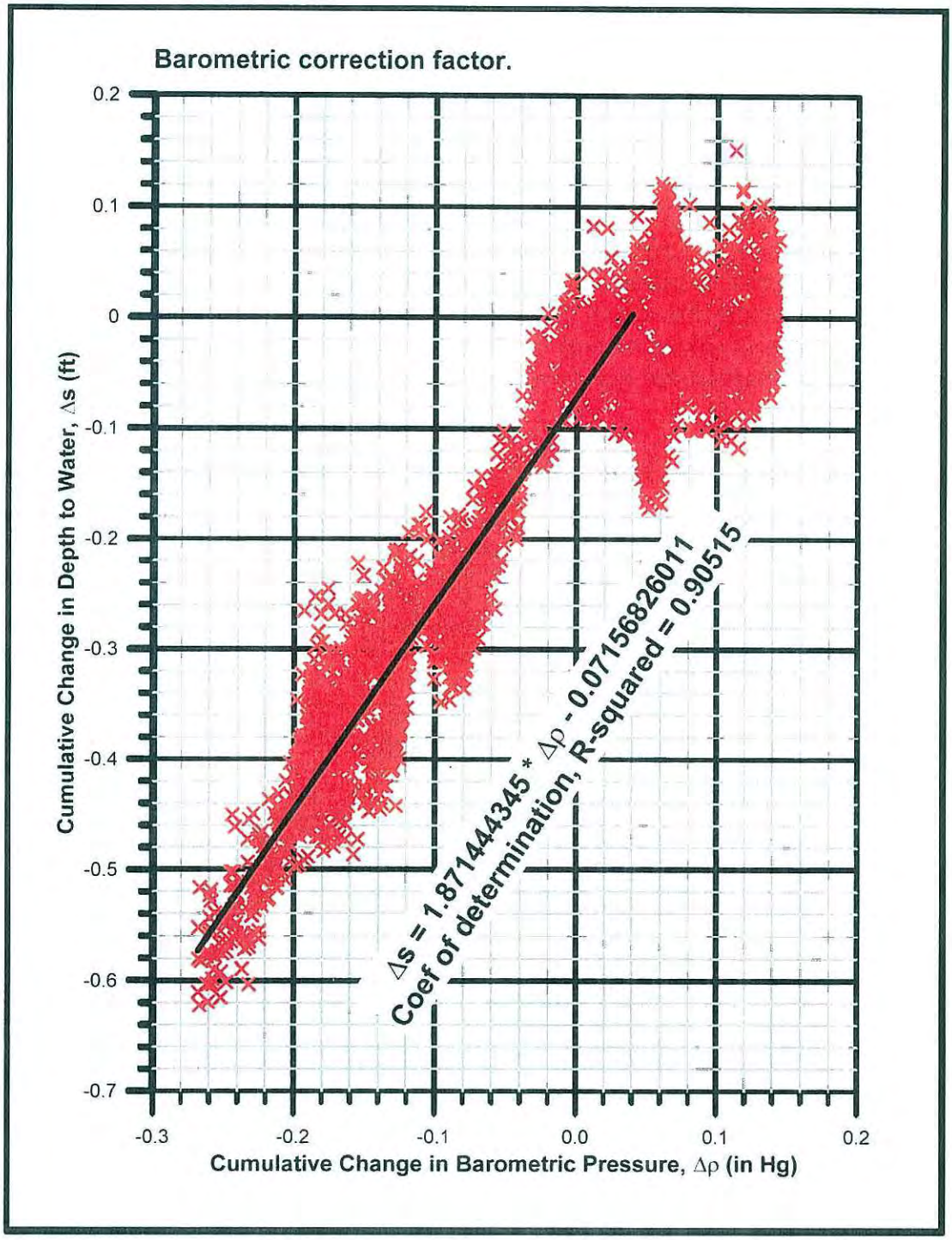

Figure 23 exhibits significant data scatter around the linear regression line, similar to the data scatter evident in the "cloud" of data to the right of the linear regression line. The data associated with the linear regression hint at a cyclical nature to the scatter.

Figure 24 shows the static water level and barometric pressure data compared to the tide at Seattle, Washington, with the tidal data adjusted to plot in the exact time zone at Test Well #2A by correcting the tide time by the degrees, minutes and seconds of longitude between the Seattle tide recorder the test well. It is evident from Figure 24 that earth tide at the test well causes a diurnal fluctuation of approximately 0.2 feet superimposed over the groundwater level observed in Test Well #2A.

The diurnal fluctuation of approximately 0.2 feet is consistent with the width of the data scatter on each side of the linear regression line on Figure 22 and is the likely explanation for most of the data scatter on Figure 22. The fluctuation of the static water level approximately 0.55 feet in response to barometric pressure change combined with a 0.2-foot diurnal fluctuation due to earth tide, as shown on Figure 24, is insignificant with respect to the drawdown of the aquifer water level during pumping and is therefore not of concern in interpretation of time-drawdown data collected during pumping tests with pressure transducer equipment that is vented to eliminate barometric effects on the instrument.

Figure 24: Static water level and barometric fluctuation compared to Seattle tide.

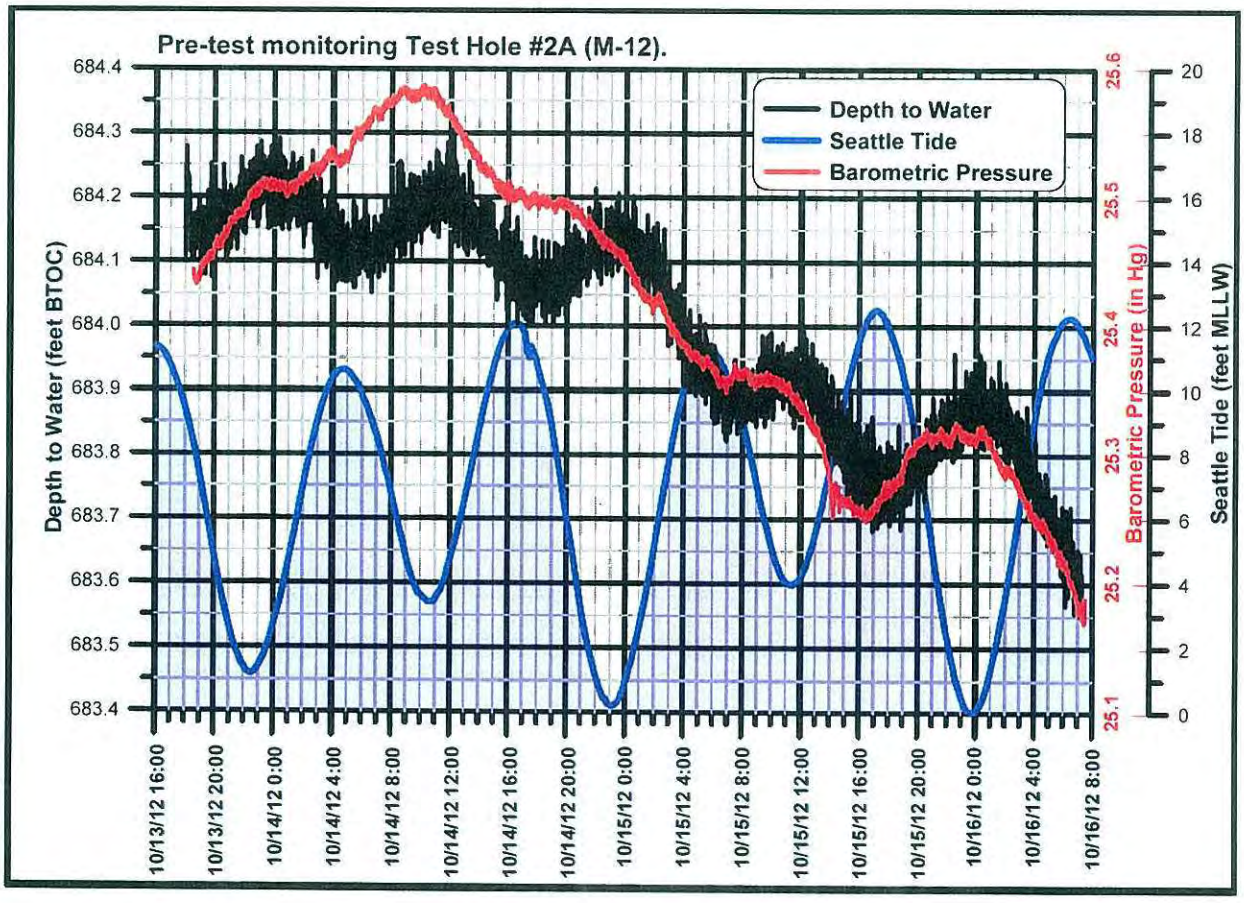

5.2 Test Pump Equipment

Two test pumps were used to pump Test Well #2A; an ESP TP1700 GE oil and gas pump which failed during the October 2012 stepped rate test and an ESP EN35000 GE oil and gas pump which operated near maximum capacity to perform the 1500-gpm test in December 2012. Pump performance curves are shown below.

5.2.1 ESP TP1700 8-Stage Pump Curves

The ESP TP1700 pump used in October was set with the inlet at a depth of 1693.26 feet BTOC in the 16-inch casing or 1689.26 feet BGL. The bottom of the pump motor was at a depth of 1770.41 feet BGL.

Figure 25: ESP TP 1700 pump performance summary.

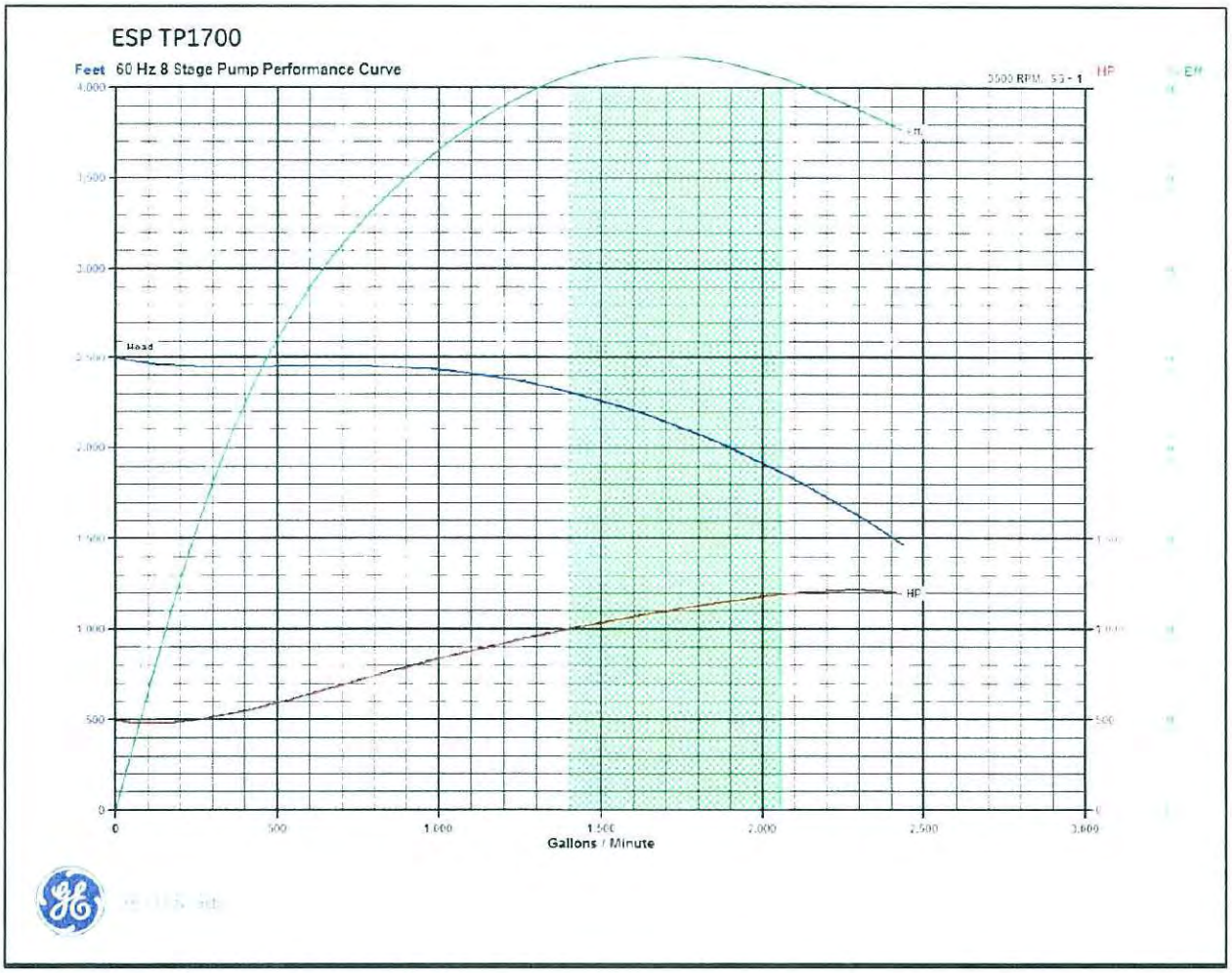

Figure 26: ESP TP1700 test pump VFD performance curves.

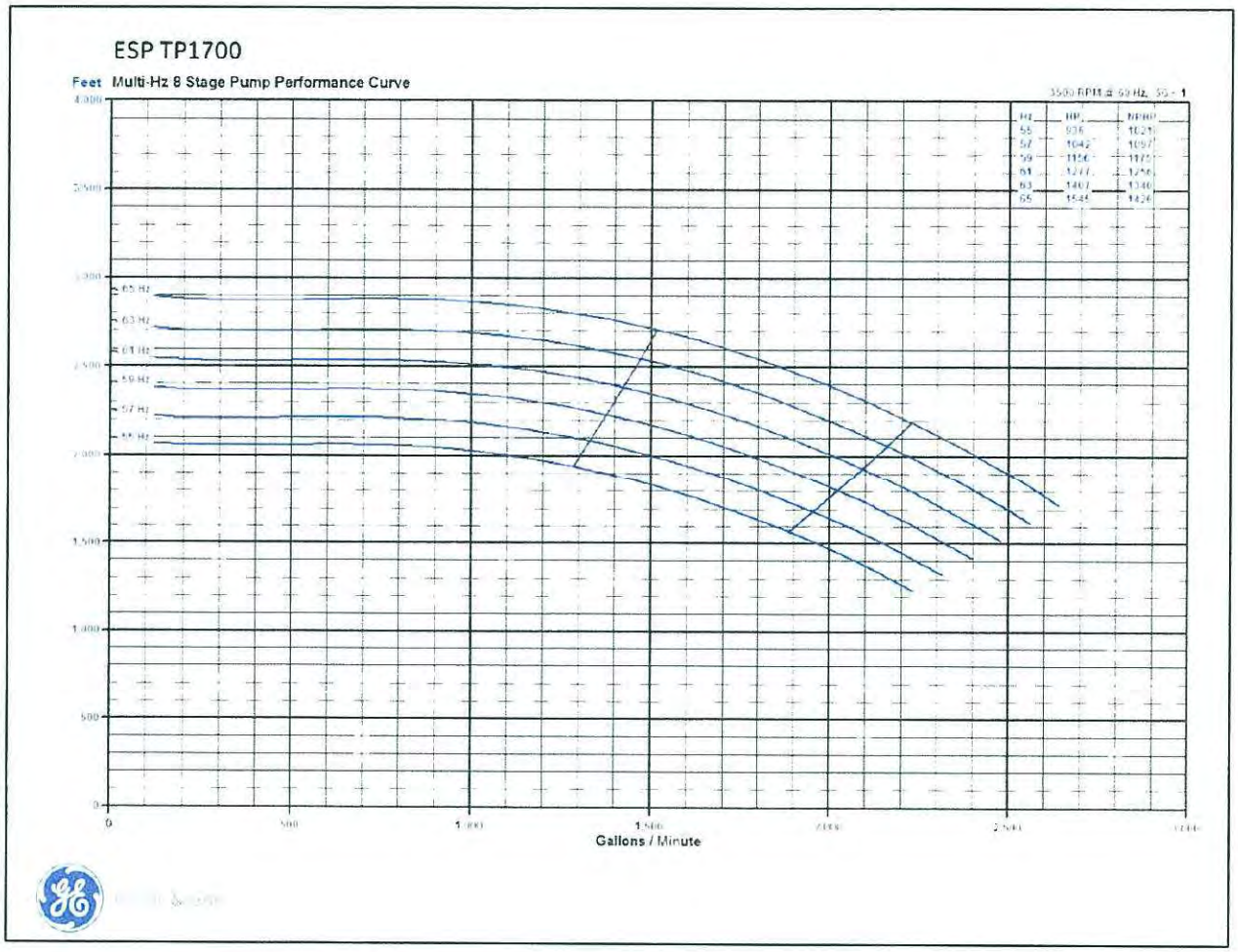

The ESP TP1700 pump was an ideal test pump for Test Well #2A, providing slightly more than 2300 feet of TDH at 60 Hz and 1400 gpm, thus exceeding the test pump specifications which required a pump capable of 1400 gpm at 60.5 Hz and 2150 feet of total dynamic head. On paper, the pump was capable of producing up to 2200 gpm at 65 Hz and 2200 feet TDH; thus affording the opportunity to test the well at rates much greater than 1400 gpm. However, the pump did not perform on the performance curves during the 510- and 650-gpm steps and the stepped rate test was ultimately stopped because of excessive vibration in the pump. The vibration indicated that the pump was faulty when it was installed. Subsequently, it was found that the bearings had failed in the lower end of the pump and impeller in the lowermost stage was failing.

5.2.2 ESP TP1700 Performance

Observations taken at the time of the October 2012 step test indicate the test pump was not performing on the pump performance curve. For example, at 10:30 a.m. on 10/21/2012, the pump column pressure at the throttling valve was set to 20 psi while the pump was discharging 510 gpm. A manual measurement of the depth to water with an

electronic water level indicator tape provided a pumping water level of 1073.20 feet below the measuring point at the top of the standpipe. The pump column pressure of 20 psi is equivalent to 46 feet of head, which added to the pumping water level, is 1119 feet. Friction loss in 6-inch pipe with a roughness coefficient of 120 is 2.417 feet per 100 feet of pipe. This provides 40 feet of head loss in 1679.45 feet of pump column, as installed for this test. Actual friction loss for 7-inch oilfield tubing used for pump column was less, however, 40 feet of friction loss is a conservatively large value. The sum of the elevation lift of 1073 feet, estimated friction loss of 40 feet, and 46 feet of pump column pressure is a Total Dynamic Head (TDH) of 1159 feet. According to Figure 26 above, the pump should deliver more than 2000 feet of TDH at 510 gpm and 55 Hz, exceeding the observed values by more than 840 feet of head. Even with the VFD reduced to 40 Hz, the pump column pressure should be more than 120 psi. Therefore, the observed data indicate the test pump was providing less than the rated pressure shown by the pump performance curves.

5.2.3 ESP TN35000 12-Stage Pump

The pump inlet of the ESP TN35000 pump used in December 2012 was set at a depth of 1755.89 feet BTOC in the 16-inch casing or 1753.49.4 feet BGL. The bottom of the pump motor was at a depth of 1835.53 feet BGL, partly in the 10-3/4 inch casing.

Figure 27: ESP TN 35000 pump performance summary.

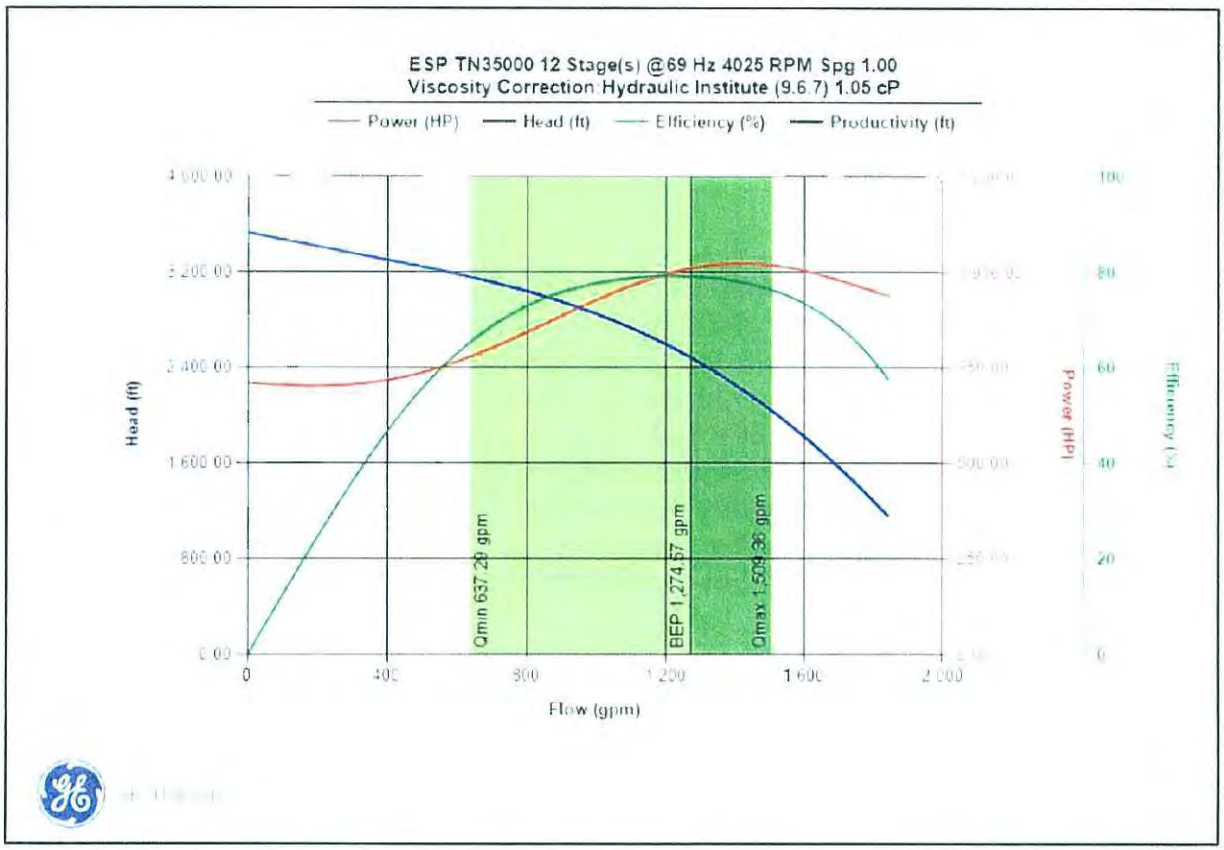

Figure 28: ESP TN35000 test pump VFD performance curves.

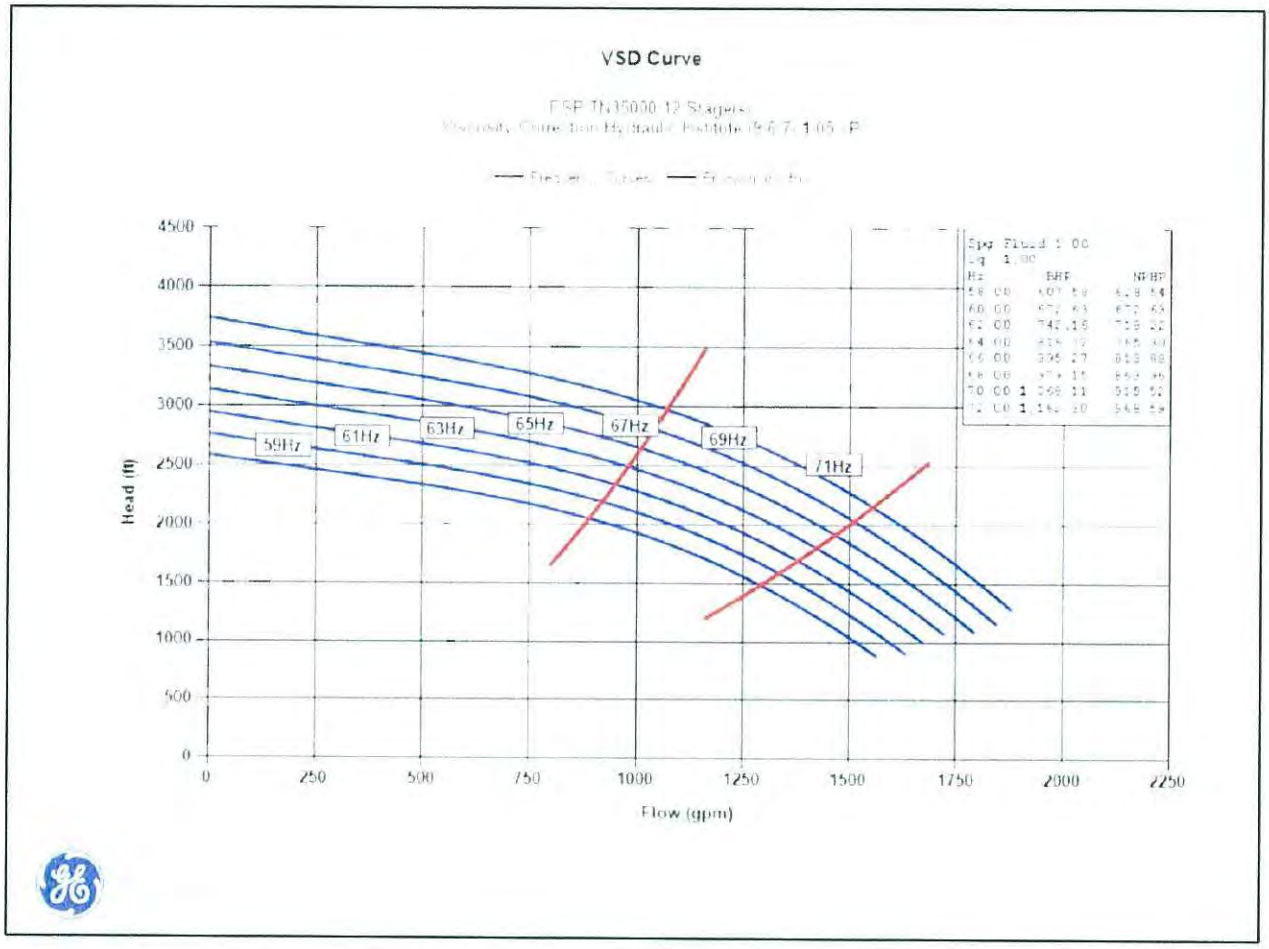

The ESP TN35000 test pump did not satisfy the specifications for a test pump which require the pump to deliver 1400 gpm at 60.5 Hz and 2150 feet TDH. As shown on Figure 28, the ESP TN35000 test pump delivers approximately 1100 gpm at 60.5 Hz and 2150 feet TDH. However, it was anticipated that acid stimulation of the well would greatly reduce the actual TDH that would be required during the pumping test. The ESP TN35000 was capable of delivering the required 1400-gpm minimum test rate at approximately 1900 to 2400 feet TDH and various VFD frequencies exceeding 60.5 Hz. The pump was accepted for the December 2012 tests on that basis, because no other test pump was available without a substantial delay for the pump to be assembled and delivered.

5.2.4 Test Pump Assembly

An overview of the well site during October 2012 pumping test is provided on Photo 96. The photo shows the portable generator housed on van trailer on the left side of the photo, the VFD unit on a flatbed trailer with a yellow equipment rack to the right of the generator, a motorized reel for the submersible pump motor cable on the far side of an SUV, a pump truck with its mast extended above the well and a pipe trailer for pump

column backed up to the well, and the 10-inch discharge pipe extending from the well, left across the pad to where it is buried in the ground to convey discharge water to the north side of the drilling pad on the far left side of the photograph.

Photo 96: Overview of Test Well #2A pumping test layout on 10/21/2012

Photo 97 shows the data plate on the secondary transformer on the Southwest Electric Co. variable frequency drive (VFD) unit (also referred to as a variable speed drive or "VSD"). The VFD is capable of delivering 2000 to 6928 volts of 3-phase power at 433 to 125 amperes with 75 kV BIL. The kV BIL rating is the basic impulse level (BIL) of the transformer and measures its ability to withstand surges.

Photo 98 shows the 5-inch diameter motor assembly hanging from the pump truck during installation. The motor assembly in Photo 98 consists of two 35.5-feet long, 500 nominal horsepower motors coupled together in a 71-foot long motor assembly.

Photos 99 through 108 show other components of the test pump assembly with explanatory photo titles.

5.2.5 Logging Equipment and Data Collection

Three standpipes were installed to the top of the test pump as shown in Photo 104. Two 500-psi In-Situ Level TROLL pressure transducers and loggers were installed, each in a separate standpipe, and the third standpipe was equipped with an electronic water level indicator with a steel tape graduated to hundredths of a foot. It was intended

Photo 97: VFD secondary transformer data plate.

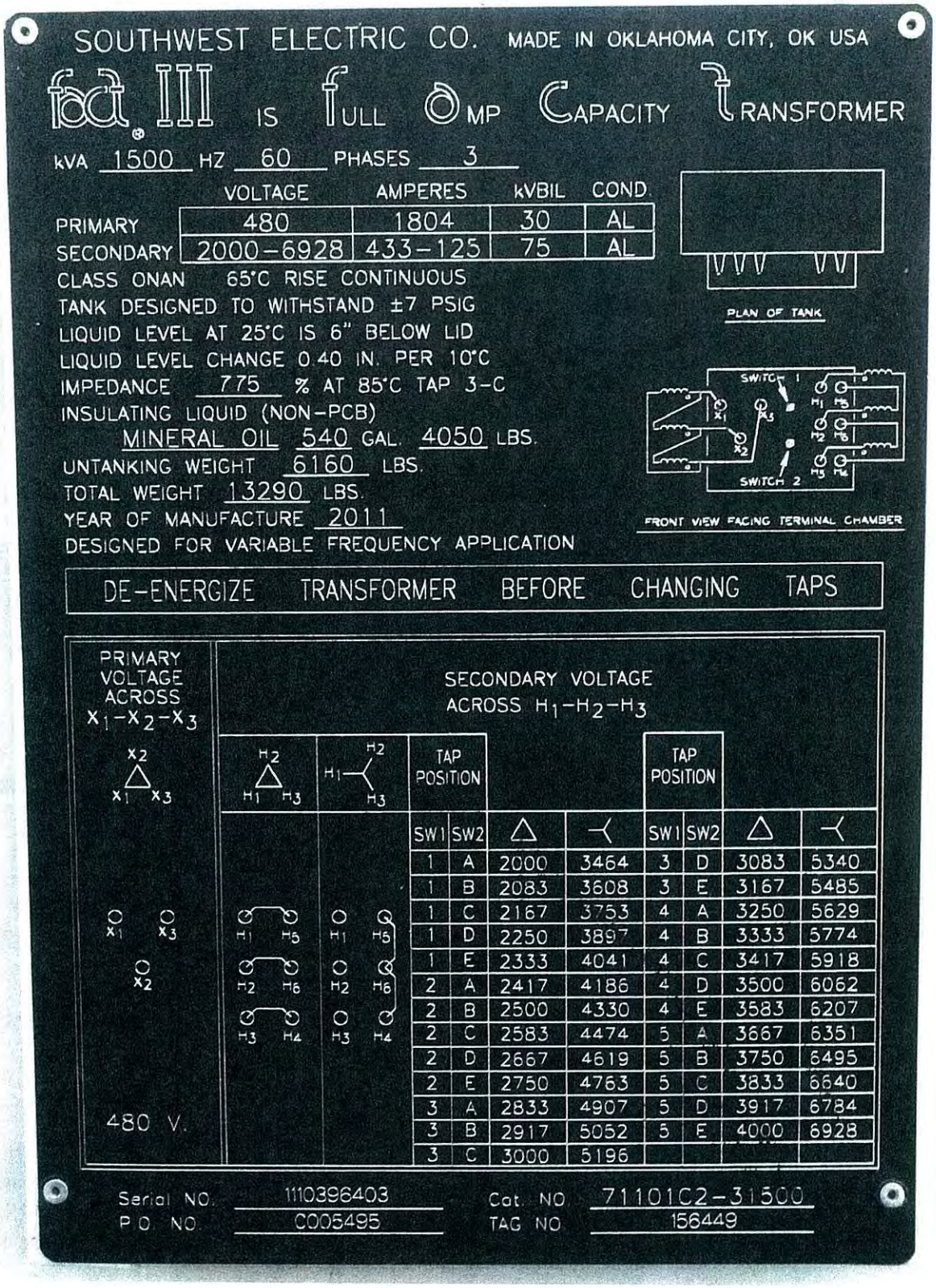

Photo 98: Motor assembly hanging from pump truck.

Photo 99: Coupling between oil seal (upper part) and motor (lower part).

Photo 100: Mounting plate for motor-to-pump connection.

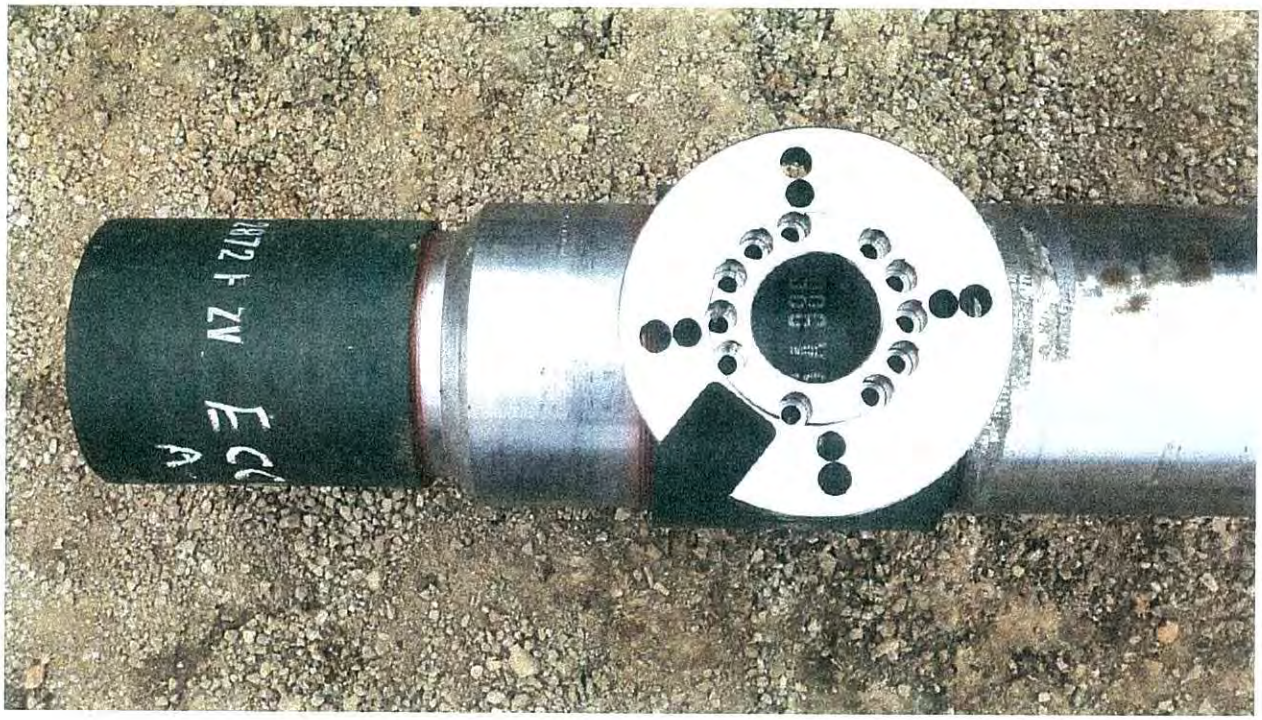

Photo 101: Pump with riser pipe hanging above motor suspended in top of well.

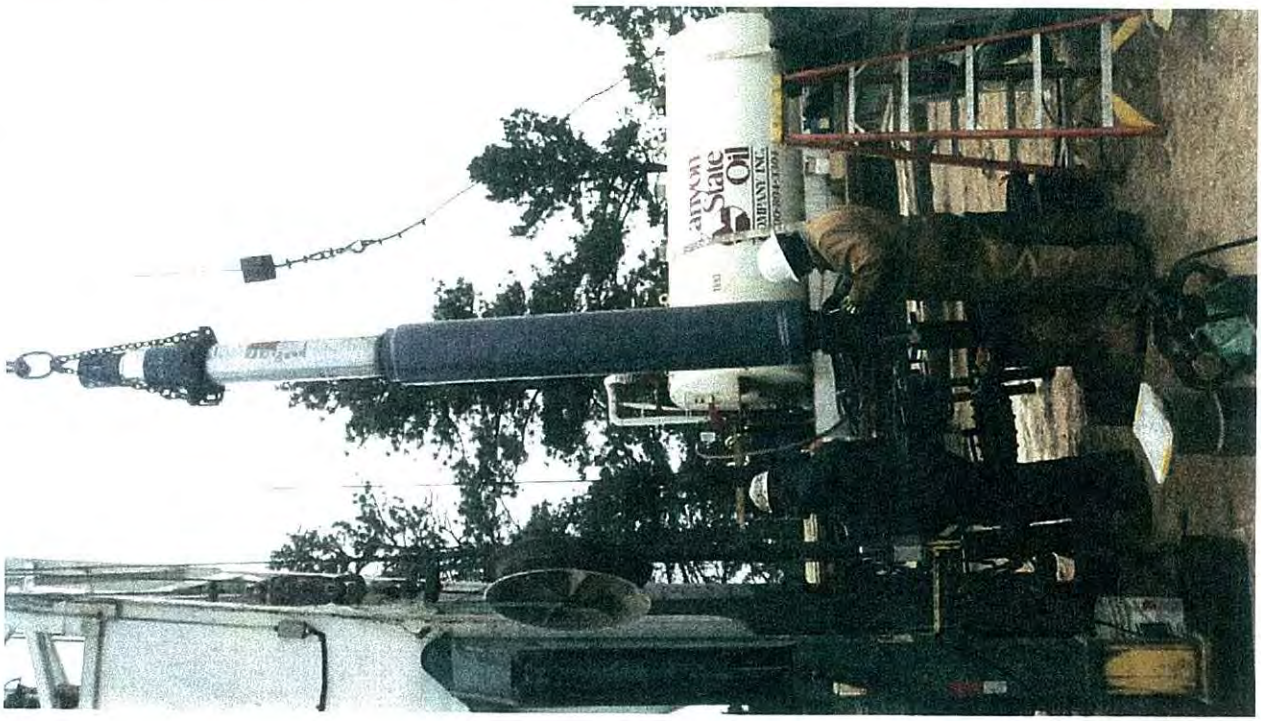

Photo 102: Pump mounting plate on motor prior to attachment to inlet section on pump.

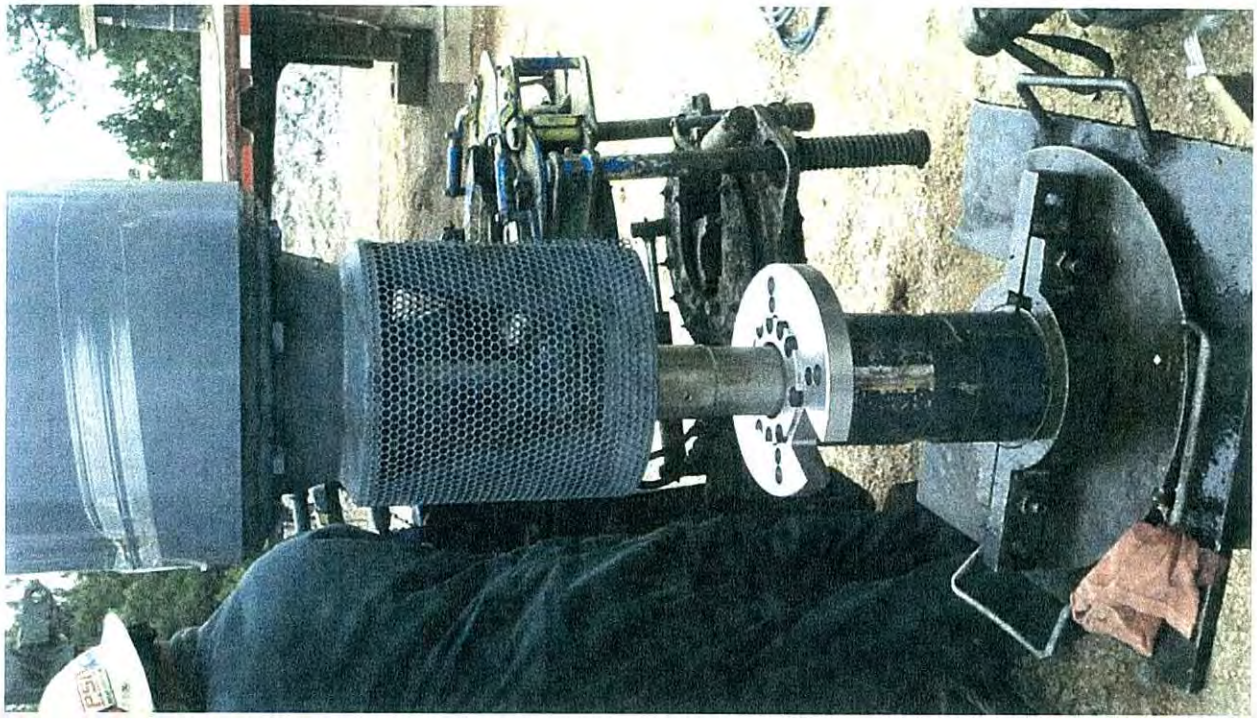

Photo 103: Motorized cable reel for pump motor electrical cable.

Photo 104: Bottom of three PVC standpipes used for well instrumentation.

Photo 105: Pump column and standpipe installation.

Photo 106: Installation of 10-inch steel discharge pipe.

Photo 107: 10-inch discharge pipe with butterfly valve and flow meter.

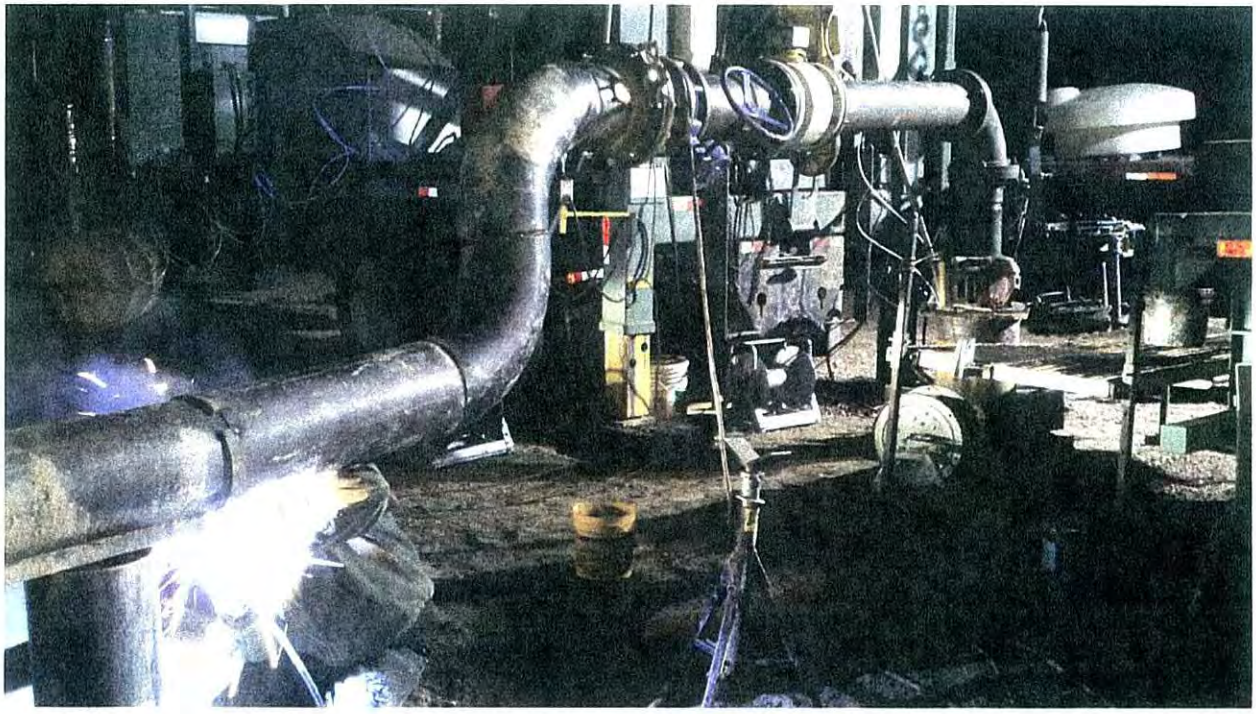

Photo 108: Well head with standpipes, two pressure transducers, water level indicator, airlines and armored electrical motor cable passing through support plate.

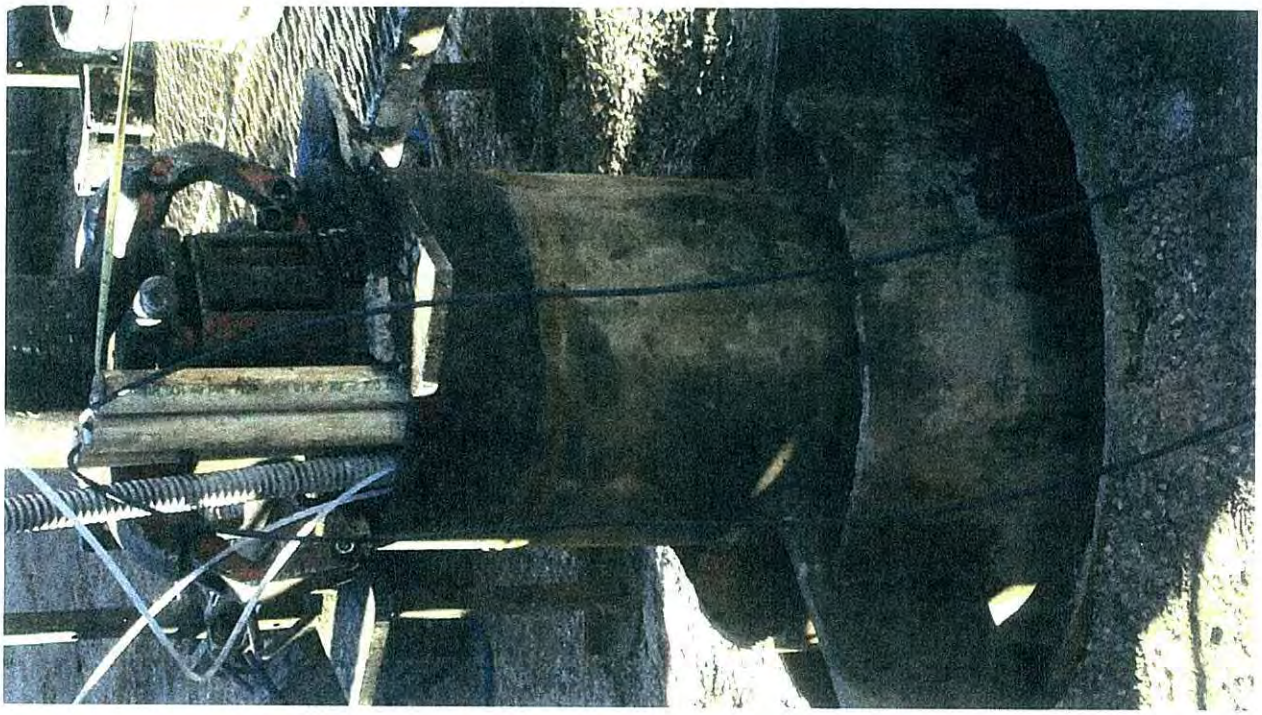

that the pressure transducers would rest on the bottom of the standpipes; however, the PVC standpipes were deformed between the pump column and the casing such that the actual depths to the pressure transducers were less than the lengths of the standpipes. One pressure transducer failed and filled with water, so no record was obtained from it.

The static pressure over the functioning pressure transducer was 429.179 psi, indicating the pressure transducer was 990.421 feet below the static water level of 689.083 feet BTOC (top of standpipe) or at a depth of 1679.5 feet in the well, below the top of the standpipe. The depth of 1679.5 feet below the top of the standpipe is equivalent to 1676.129 feet BGL or 13.131 feet above the pump inlet. The Level TROLL 700 equipment was programed to collect depth to water, pressure on transducer and water temperature at a one-minute frequency for all tests.

5.3 October 2012 Pumping Test

The stepped rate test of Test Well #2A started on 10/18/2012 using the 8-stage ESP TP1700 pump. The test pump was installed by noon and the pump was started at 1:23 p.m. for an intended pumping rate of 500 gpm. The limits within which the flow meter feedback loop would control the VFD pumping rate had not been fine-tuned and the discharge rate was surging way out of limits for test, so pumping was stopped at 1:27 p.m. to reprogram the PLC receiving the flow meter signal.

Pumping resumed at 1:45 p.m. with an initial flow meter rate of 881 gpm which was 575 gpm by 1:46 p.m. and then 500 gpm with a surge of about 100 gpm as the drive was further fine-tuned, reducing the surge to about 40 gpm by 1:56 p.m. and to 15 gpm by 2:00 p.m., with surge nearly eliminated by 2:06 p.m at a rate of 508-509 gpm. The generator quit at 2:08:50 p.m. A second attempt at a 500-gpm step was attempted starting at 3:15 p.m., however, after replacing all four thermostats the diesel motor on the generator continued to overheat, due to plugged cooling fins on the radiator. This was a new generator with 18 hours of total run time; however, the radiator fins were found plugged with dust and flying insect remains. By late evening of 10/18/2012, a replacement generator was dispatched from Albuquerque, New Mexico, which was the nearest available generator of adquate size.

On 10/21/2012, with the replacement generator connected, pumping was initiated at a 500-gpm rate at 8:00 a.m.; however, pumping was stopped at 8:15 a.m. due to the amount of vibration in the pump column. At 8:45 a.m. the pump was operated with the VFD control switched for reversed rotation and the pump did not vibrate; however, the motors pulled full amperes and volts; indicating the pump was turning backwards, as indicated by the rotation direction signal on the VFD. The pump was stopped at 8:48 a.m. and the well was allowed to recover until 9:10 a.m. when the pump was started at the 500-gpm rate. The gasket on the discharge elbow at the top of the pump column failed and the pump was stopped at 9:11 a.m. to replace the gasket. Pumping was started again at 9:40 a.m., and the VFD was adjusted to ramp up the pumping over a longer period of time to avoid surge on the gaskets in the discharge pipe. The pump and pump column continued to vibrate to the extent it was hard to read the graduations on the glass on the Rossum sand tester. At 10:00 a.m. the pressure in the pump column was reduced from 30 psi to 20 psi in an unsuccessful attempt to reduce the pump vibrations.

By 10:00 a.m., polling of the pressure transducer indicated 8-foot fluctuations in the water levels measured and recorded by the logging equipment and by 10:13 a.m. this increased to 12 feet of fluctuation. At 10:30 a.m., a manual measurement with an electronic water level indicator indicated surge of about one foot as contrasted to the pressure transducer readings. Apparently the problem causing vibration in the pump was also sending pressure waves into the well, recorded by the pressure transducer as pressure fluctuations, but which caused physical fluctuations in the pumping water level of only about one foot. This is the most likely explanation for the data scatter in the pumping test time-drawdown plot.

The pumping rate was increased from 510 gpm to 650 gpm at 12:40 p.m. and pumping continued until 1:01 p.m. when the pump was stopped due to the excessive vibration and fear of a mechanical failure of the pumping equipment and/or loss of equipment in the well. Figure 29 shows the time-drawdown curves for both stepped rates. The drawdown exhibits the influence of a recharge boundary after approximately 20 minutes of pumping at the 510-gpm rate. A calculation of an apparent transmissivity (T) and hydraulic conductivity (K) are shown on Figure 29; however, they do not represent the

true transmissivity and hydraulic conductivity of the aquifer because they are influenced by recharge.

Figure 29: Time-drawdown plot of 10/21/2012 stepped rate pumping test response.

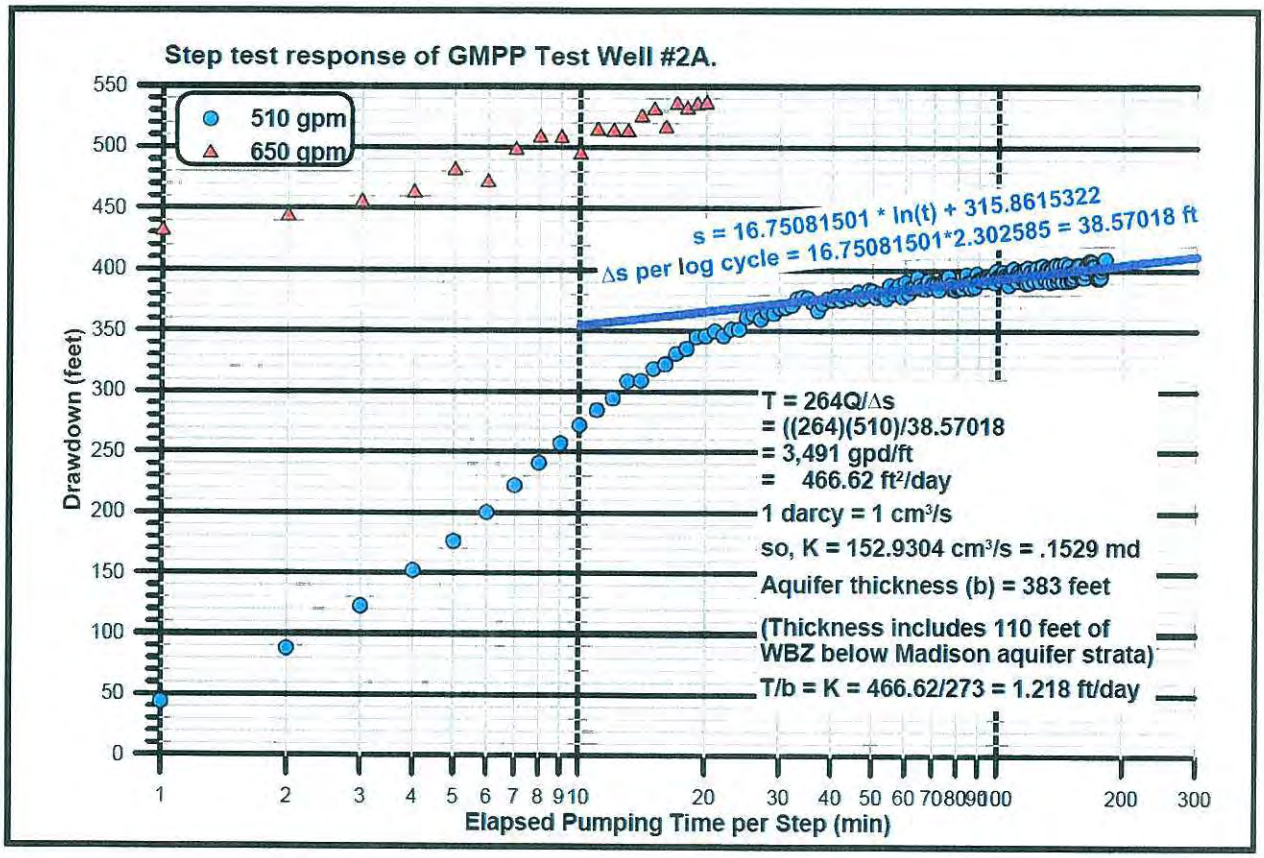

5.4 November-December 2012 Pumping Tests

After the well was stimulated with acid, a stepped rate test was conducted on 11/30/2012. Before and after the stepped rate test, best management practices were implemented to mitigate potential erosion in the natural coulee where water was discharged during the tests. After hay bales were installed at a number of locations in the bottom of the coulee, two hours of pumping were conducted on 12/2/2012 at an initial 1500 gpm, which was increased to 1600 gpm after 19 minutes, to test the effectiveness of the erosion control measures. After the well recovered from the latter pumping, a constant rate test was conducted beginning at 9:00 a.m. on 12/3/2012 and continuing uninterrupted for 2 minutes short of 48 hours when the diesel motor driving the electrical generator quit running.

5.4.1 Post-Acid Stepped Rate Test

Figure 30 shows the drawdown for each of five pumping rates plotted versus semilogarithmic time during the post-acid stimulation stepped rate test of Test Well #2A. Each step of the test was conducted for 180 minutes duration and with the pumping rate

increased between steps without ceasing pumping. Linear regression lines through the drawdown data after 70 minutes pumping time for each step show the rate of drawdown was continuing to change within the three-hour duration of each step. Derivation of well loss coefficients for use in predictive equations requires that a constant rate of drawdown be established in each step of a stepped rate test for a valid solution. Therefore, it is not valid to determine well loss coefficients for Test Well #2A from the stepped rate test. Steps of three hours duration were selected as the largest practical time per step consistent with the project time and budget limitations.

Figure 30: 11/30/2012 stepped rate test time-drawdown plots.

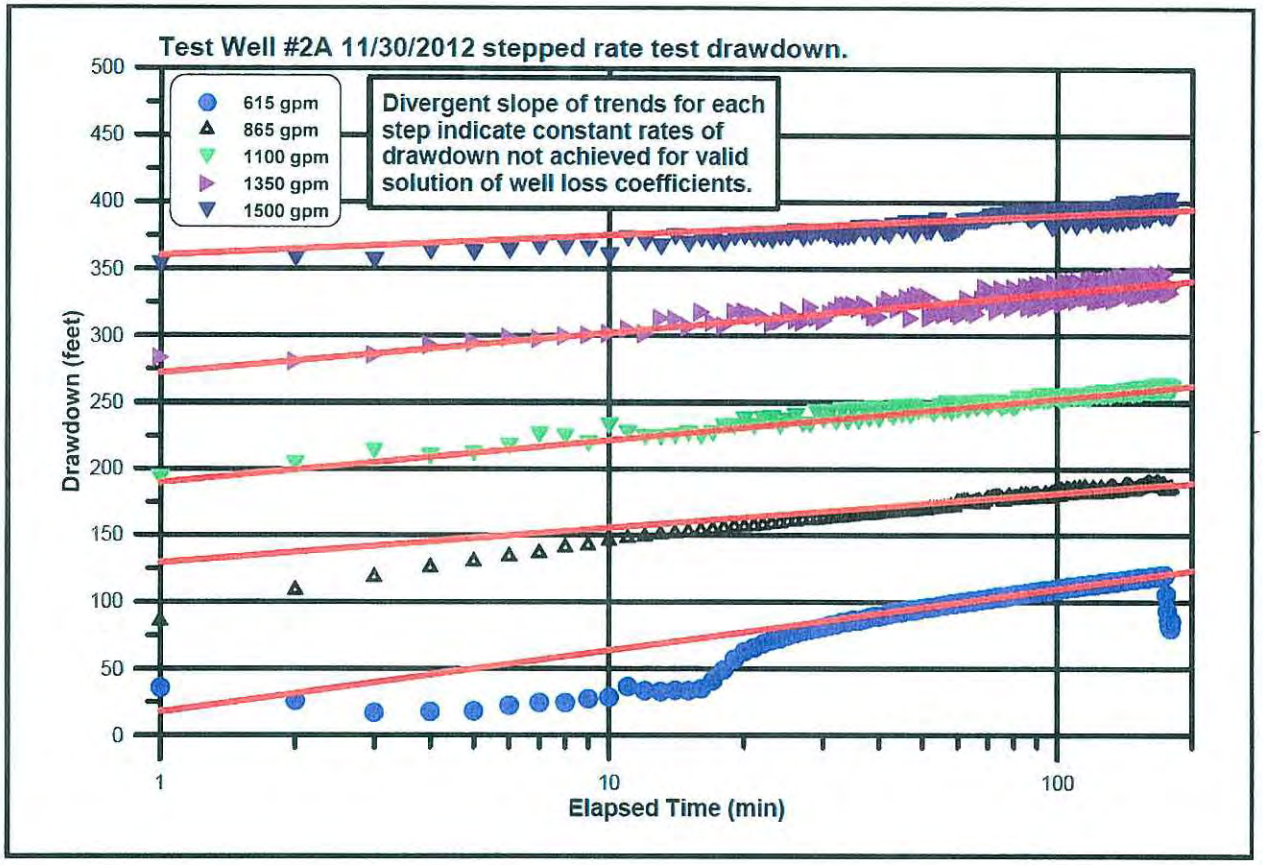

Figure 31 is another type of plot of the stepped rate data where specific drawdown is plotted versus adjusted time determined by the Birsoy-Summers (1980) method. It is evident that the 615-gpm step did not result in significant well loss drawdown and would have required many more hours to reach an essentially constant rate of drawdown, the necessary time perhaps exceeding 24 hours for that step. The latter conclusion is evident in the large separation between the 615-gpm step curve and the other steps as well as the difference in the trend of the specific drawdown with adjusted time.

Although the remaining steps of the test plot closer together on Figure 31, it is evident that they are not congruent. The trend of the specific drawdown of each step is different

and each step requires a longer period of pumping before all of the step trends will be congruent and parallel on the plot. Accordingly, no attempt is made to derive well loss coefficients from the step test data.

Figure 31: Birsoy-Summers plot of 11/30/2012 stepped rate test of Test Well #2A.

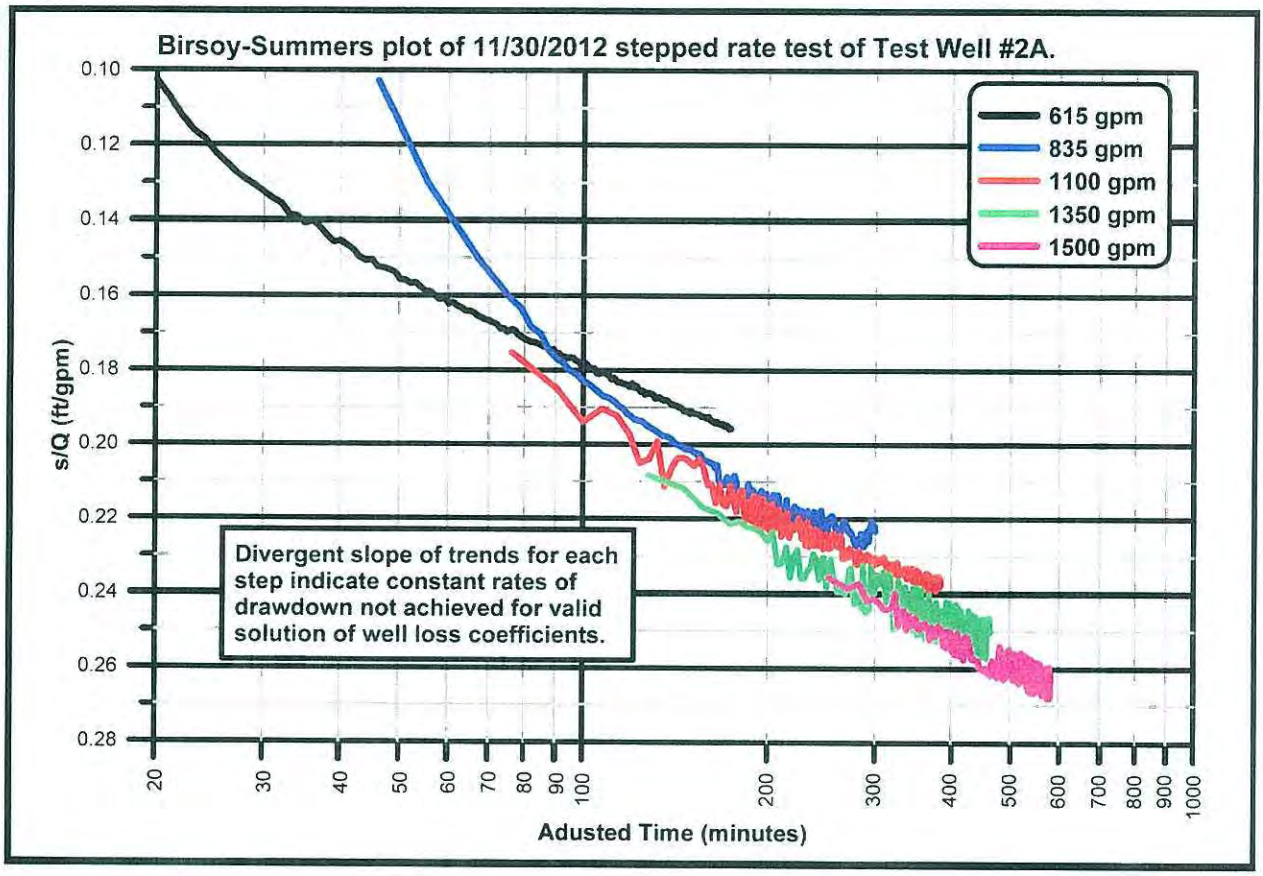

An alternative to deriving well loss coefficients to evaluate the hydraulic performance of the well is to examine the specific capacity of the well at different pumping durations. Specific capacity is unit drawdown, for example, gallons per minute per foot of drawdown and is an arbitrary, but constant standard, with which to compare performance between different wells or between different rates in a single well. Figure 32 shows the specific capacity for Test Well #2A after three hours of pumping; i.e., at the end of each 180-gpm step.

The earlier conclusion that the first step at 615 gpm did not generate much well loss component of drawdown is confirmed by the divergence of the specific capacity at 615 gpm from the trend of the other four pumping rates. The 835- through 1500-gpm rates plot on a trend that could be projected, within reasonable limits. The specific capacity curve must be defined for a specific pumping duration because it is a function of drawdown and drawdown increases as the pumping duration increases. The specific capacity is greater at early pumping times and smaller at large pumping times. The

constant rate test data are used to show the 48-hour specific capacity at 1500 gpm on Figure 32 for comparison with the 3-hour specific capacity. Although there is a temptation to shift the 3-hour curve down to the 48-hour point, it would not be a valid representation of the 48-hour specific capacity for rates other than 1500 gpm, because the drawdown rates are changing differently at three hours than at 48 hours. Even so, the specific capacity curve on Figure 32 is useful for determining the 3-hour specific capacity for pumping rates between 800 and 1600 gpm. The 48-hour point shows approximately how much increased pumping duration affects the specific capacity.

Figure 32: 3-hour specific capacity curve for Test Well #2A.

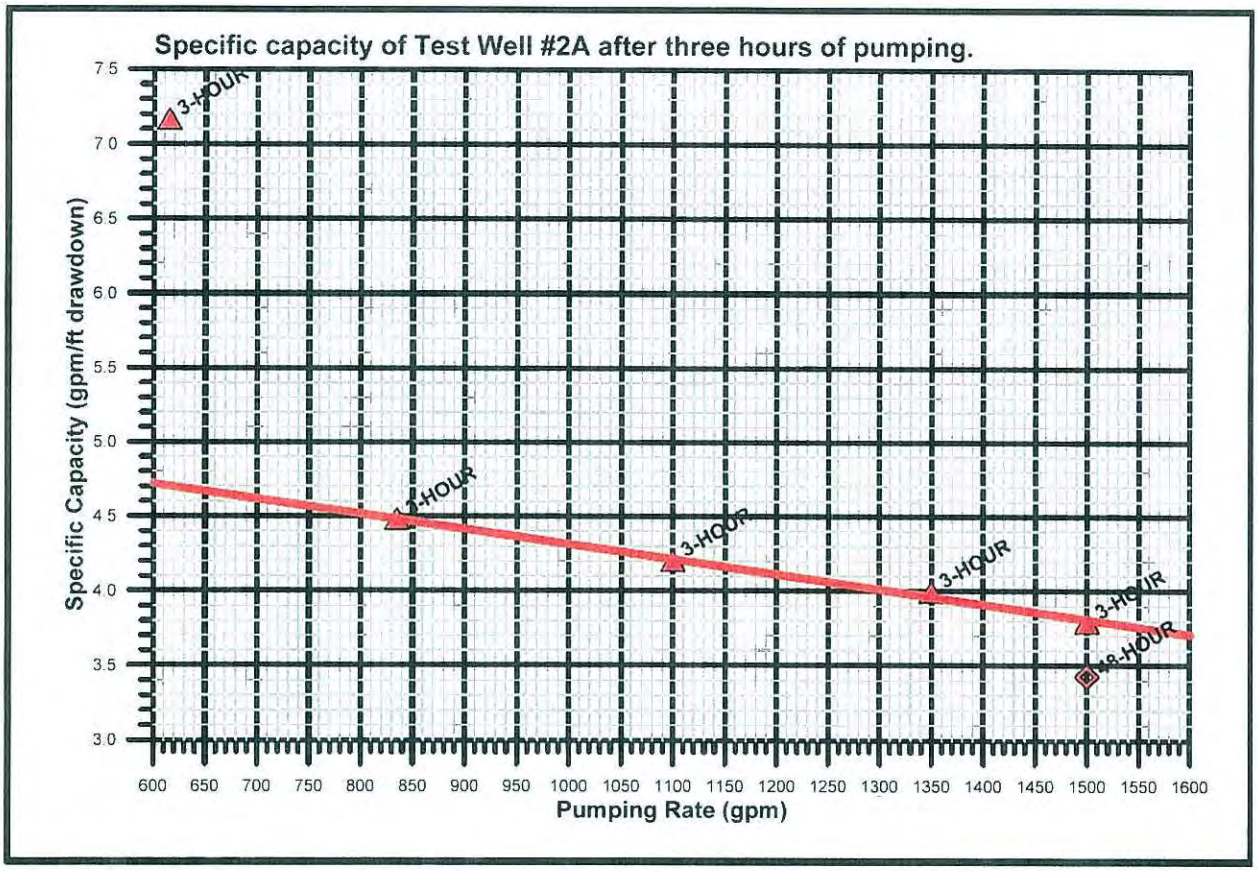

5.4.2 Post-Acid Constant Rate Test

The well was equipped with two In-Situ, Inc. Level TROLL 700 pressure transducers and loggers, as previously described, one of which malfunctioned during the test. Independent measurements of depth to the pumping water level were taken to verify pressure transducer data. The rate of flow was measured by a SITRANS F M MAGFLO MAG6000 flow meter, serial number 7ME692 677715N208 with a MAG51002 DN200 sensor, serial number 7ME658 066601D230. Full scale flow for water was 152.778 l/s (2421.5 gpm) and as shown on Figure 33, the meter was calibrated for 690 to 2072 gpm.

Figure 33: Calibration report for pumping test flow meter.

SIEMENS **CALIBRATION REPORT**

SITRANS F M MAGFLO

Customer			
Converter type	MAG 6000	Serial No.	7ME692 6777 5N208
Sensor type	MAG5100W LIN200	Serial No.	7ME658 0666 01D230
Cal. Factor	31.54572		
System Serial NO.	7ME658 0211 01U-40		

Calibration Data

Full scale flow	152.7778 l/s	Calibration liquid	Water
		Calibration rig	BG2

Calibration Settings

Frequency output	0-10000 Hz

Calibration Results

Test No.	Full scale flow	Water Temp	True Flow-Rate	Flowmeter Frequency output		
				Output	Flowrate	Error
	[%]	[°C]	l/s	[Hz]	l/s	[%]
1	100	-1.9	130.7245	8543.806	130.5304	-0.15
2	100	1.9	130.6698	8550.218	130.7658	0.07
3	25	1.9	43.5688	2854.120	43.6046	0.08
4	25	-1.9	43.5416	2855.082	43.6193	0.18
5						
6						
7						
8						
9						
10						

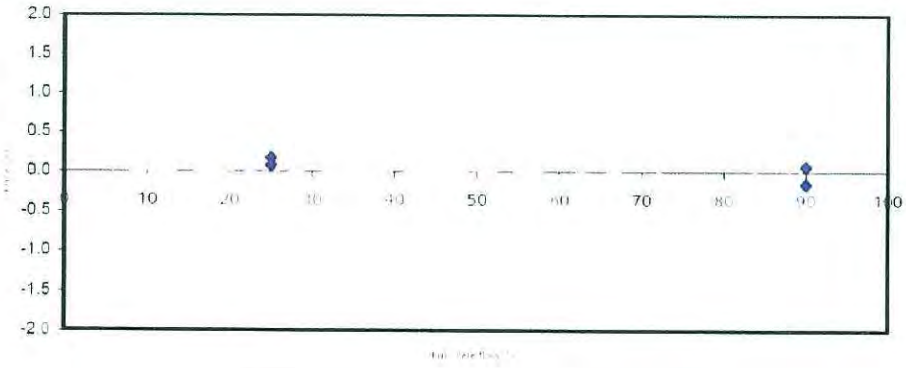

Calibrated by	hwl		
Date	2010-07-12	Time	07:42:00

The discharge rates during the stepped rate and constant rate tests were controlled by the flow meter which sent an analog signal to a PLC on the VFD controller to maintain a constant rate of flow for programmed rates. Pump column pressure was regulated by a gear-operated butterfly valve downstream from the flow meter.

A 1500-gpm constant rate test was initiated at 9:00 a.m. on 12/3/2012 and ended 12/5/2012. Figure 34 shows the 1500-gpm constant rate test drawdown response compared to the barometric fluctuations during the test. Since the drawdown is extremely large with respect to any potential effect of atmospheric pressure fluctuation, any effects of barometric pressure fluctuation are not discernible or significant to the shape of the time-drawdown curve.

Figure 35 is a diagnostic semilogarithmic plot of drawdown versus time and residual drawdown during recovery versus t/t' where t is time since pumping started and t' is time since pumping ended. The data for approximately the first 150 minutes of pumping describe a semilogarithmic straight line which is diagnostic of radial flow. After 150 minutes of elapsed pumping time, the rate of drawdown begins to decrease and departs from the projection of the earlier straight-line response. The difference between the straight-line response and the observed data is high-lighted in blue on Figure 35 and called out as "Recharge". The recharge effect also appears toward the end of recovery from pumping, when the residual drawdown departs from the straight-line response beginning at t/t' equal to about 7.0.

The "Corrected Drawdown" represents the observed drawdown minus well loss. Determination of well loss is shown on Figure 36. When well loss is subtracted from observed drawdown, that portion of the observed drawdown subject to recharge effects is shifted downward, making the corrected drawdown plot below the actual observed residual drawdown during recovery. The difference between the corrected drawdown and observed residual drawdown is simply a mathematical result of the correction for well loss and has no significance to the recovery of the water level in the well.

The significance of Figure 35 is that the Madison aquifer at this location provided a radial flow response, not one controlled by a large solution-enlarged fracture, despite the fact an earlier attempt to drill a well on this site hit a large vertical fracture in the Minnelusa, thus creating an expectation of linear flow response due to a corresponding fracture in the Madision limestone. Furthermore, the onset of recharge to the cone of depression around the pumped well requires an explanation of the source of recharge.

Figure 36 shows that the well loss component of the drawdown observed in the well is 154 feet at the 1500-gpm pumping rate. When pumping stops, the well loss component of drawdown dissipates essentially instantaneously, and the residual drawdown during recovery is all due to removal of groundwater from storage with no additional component of drawdown due to vertical flow near the well or friction loss in the formation near the well, all of which contribute to well loss drawdown during pumping. The difference between drawdown and residual drawdown is therefore equal to the well loss.

Figure 36 also shows a conventional Cooper-Jacob semilogarithmic straight-line solution for aquifer transmissivity, producing a result of 3336 gpm/ft or 446 ft^2/day. The solution for transmissivity is derived from that portion of the data prior to the onset of the recharge boundary. The rate of drawdown at the end of the constant rate test was changing fast enough that it cannot be accurately predicted by a mathematical projection of the late time-drawdown data, based on regression analysis on a log-log plot; however, a different type of plot allows prediction of future drawdown based on regression analysis, as shown on Figure 37.

Recovery of water levels in the well between pumping cycles is important. In order to assess the rate of recovery from the 1500-gpm test, it is necessary to note that when the pumping duration of the test is equaled by the duration of the recovery time after the test pumping stops, the value of t/t' will equal 2.0. The test data (Figure 36) show that when t/t'=2, residual drawdown is 4.975 feet; i.e., two days of recovery after two days of 1500-gpm pumping, the water level in the aquifer at the well remains 4.975 feet below the original static water level.

Residual drawdown is accumulative. For example, if the well is pumped two days on and two days off for an 80-day period in the summer, residual drawdown will accumulate for 20 pumping cycles. Twenty pumping cycles times 4.975 feet of residual drawdown per cycle totals 99.5 feet of residual drawdown at the end of the 80-day pumping period. Thus, accumulated residual drawdown at the end of one season of pumping can be significant.

In this hypothetical example, the well would have 285 days to recover, or 3.56 times the duration of the season of use. This will allow all or most of the 99.5 feet of accumulated residual drawdown in this example to recover before the next pumping season. If we look at another hypothetical, we might assume that after recovering for 285 days, 1.5 feet of residual drawdown remains. If this pattern is repeated 20 times for 20 years of pumping, the residual drawdown at the end of 20 years will be 30 feet and the operator of the well field will observe static water levels in the well that are 30 feet deeper than when the well was new 20 years earlier.

It is not suggested herein that the above hypothetical will take place, but it does point out the need to evaluate the potential for long-term drawdown based on a realistic assessment of the likely future use of the well.

Figure 37 shows the time-drawdown data plotted as arithmetic drawdown versus the square root of elapsed pumping time. A semi-logarithmic regression analysis of the data from square root 45 (2025 minutes elapsed pumping time) through the end of the data provides an equation that can be used to make a reasonably conservative projection of the rate of drawdown into the future, taking into account the trend of the drawdown near the end of the test. Projection of the drawdown to square root 100 (10,000 minutes or 6.94 days) provides an estimated drawdown of 459 feet. Projection

Figure 34: Barometric fluctuation compared to drawdown.

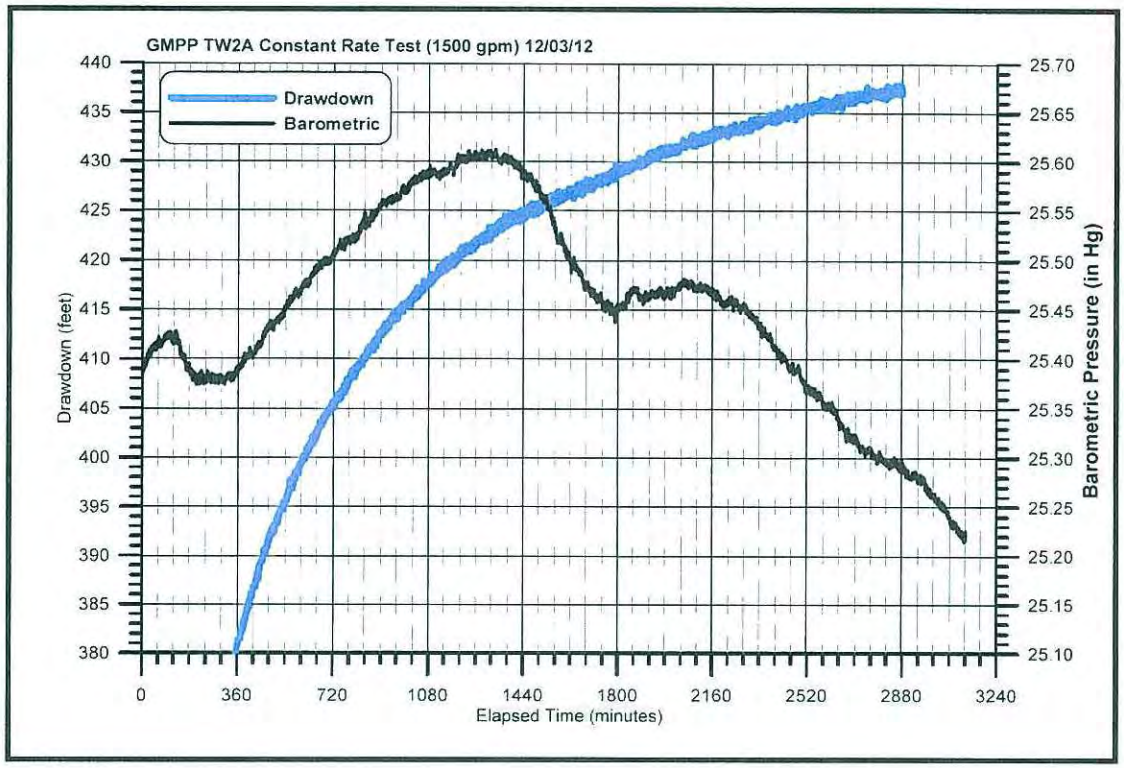

Figure 35: Semilogarithmic time-drawdown plot of 1500-gpm test of Test Well 2A.

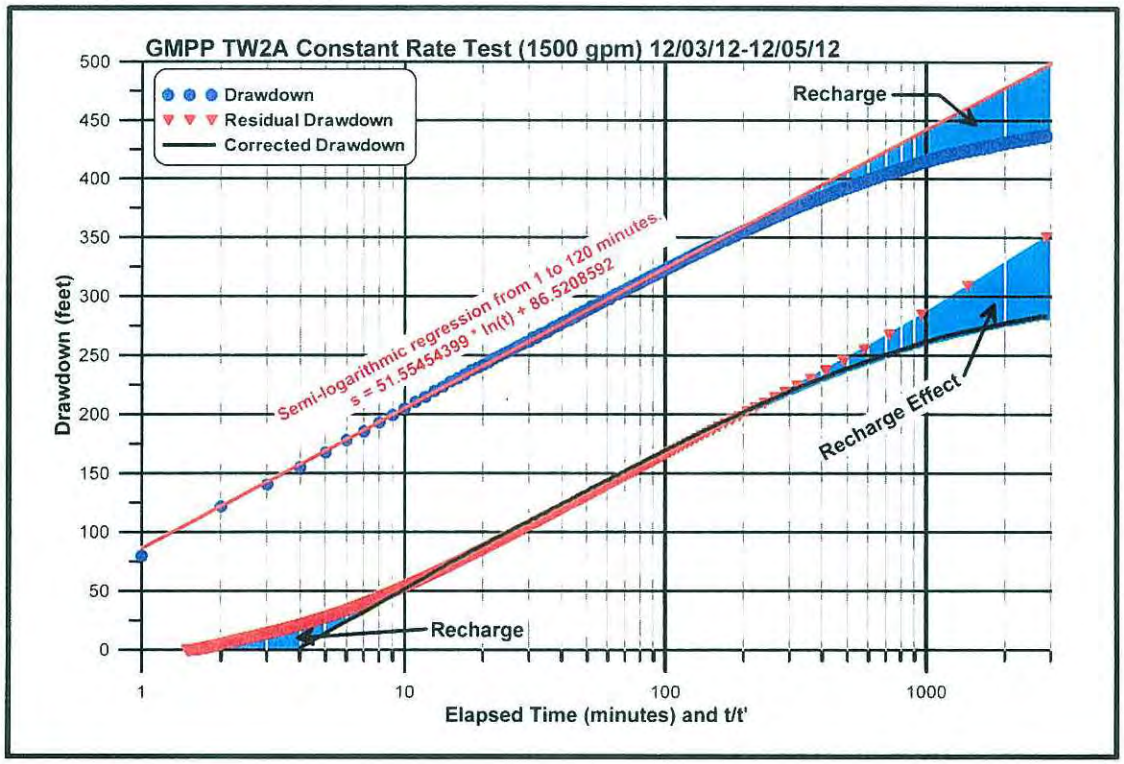

Figure 36: Cooper-Jacob solution for transmissivity and determination of well loss.

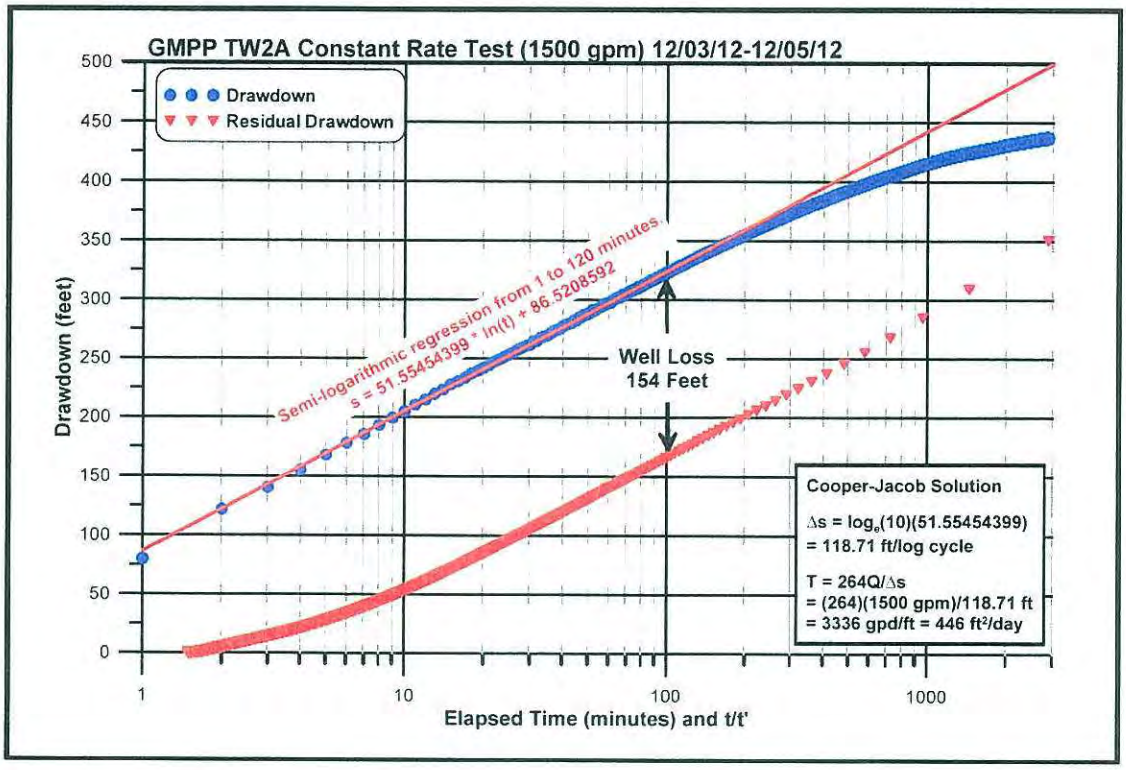

Figure 37: Drawdown plotted versus square root of time for projecting drawdown.

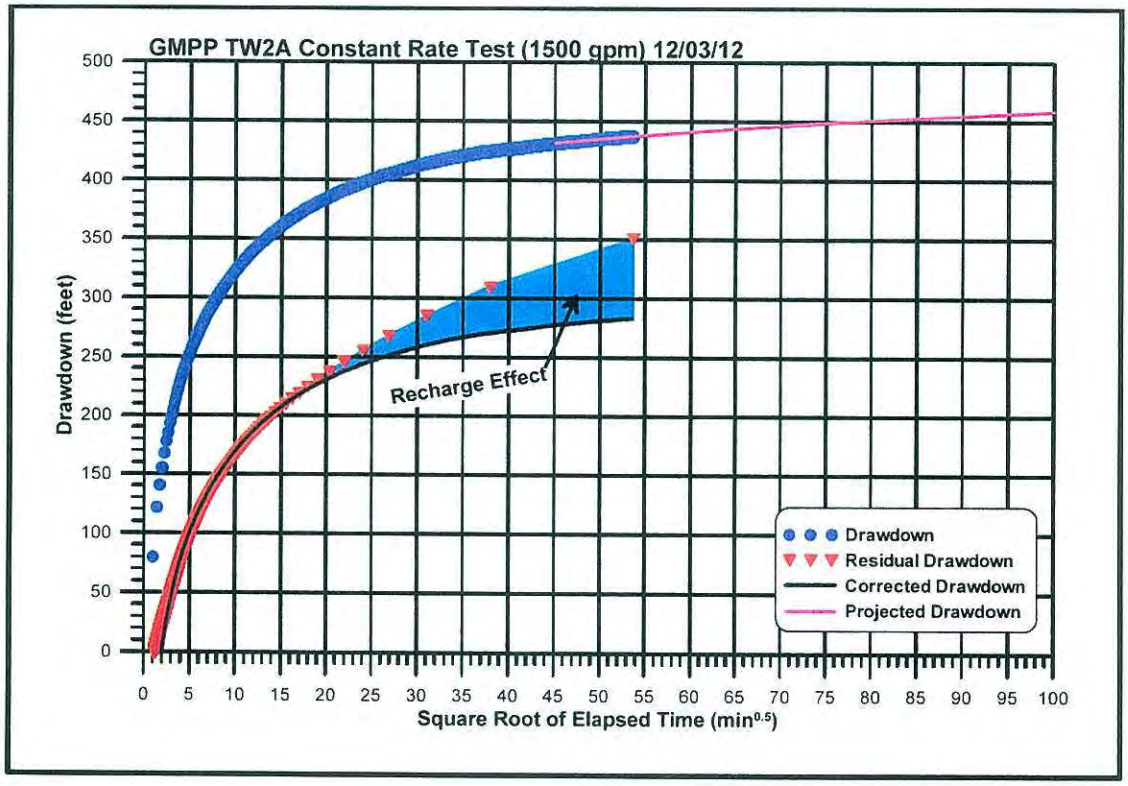

of the drawdown to 70 days of continuous pumping at 1500 gpm (not shown on graph), results in a predicted drawdown of 498.6 feet. Projection of the drawdown to two years (square root 1025) continuous pumping at 1500 gpm, results in a predicted drawdown of 539 feet. It is therefore concluded that this well can be pumped at 1500 gpm for long periods of time without causing excessive drawdown of the water column available above pump inlet settings in the lower part of the 16-inch casing which is open for pumps to 1795 feet.

The projection on Figure 37 is important because it provides a means to assess the potential for long-term drawdown at the well, as affected by recharge, a projection that could not be made as comfortably from Figure 36. The R-squared value for the fit of the semi-log regression through the data from square root 45 to the end of the data (2025 minutes to 2878 minutes) is 0.977.

The foregoing analysis provides a value of aquifer transmissivity as well as a means of projecting future drawdown, even though the aquifer response during the test is affected by a source of recharge that causes the test data to depart from the mathematical model for ideal radial flow to a pumped well. This raises the question of what is providing the recharge to the cone of depression around Test Well #2A during the aquifer test. The answer to this and other information is provided by the response of existing well M-1 (Figure 1) to the pumping during the test.

Figure 38 shows hydrographs of the water levels measured in existing wells M-1 and M-2 by the City of Gillette SCADA systems for those wells. The elevations of the two wells were obtained from Google Earth. The groundwater elevations in the two wells are likely closer together than shown on the graph, but the separation was left as shown on the graph to help distinguish between and compare the two hydrographs. As shown by the graph, the M-1 well in particular exhibited a strong response to the test pumping at TW#2A.

The distance between pumped well TW#2A and M-1, as measured on Google Earth, is 2785 feet. Likewise the distance between pumped well TW#2A and M-2 is 3600 feet. Figure 39 shows the response of the furthest well, M-2, to the 1500-gpm pumping rate. The drawdown at the well is so small that the smallest value recorded, 0.0006 feet, is observed only after more than one day of elapsed pumping time. The maximum drawdown after two days of pumping is 0.30 feet. Accordingly, use of a new production well completed at TH2A is not a matter of concern with regards to causing excessive drawdown at well M-2.

Figure 40 is a semilogarithmic time-drawdown plot of the response of well M-1 to the 1500-gpm pumping test for two days at TW#2A. The acceleration of the three different segments of the time-drawdown response is indicative of highly bounded flow. The large delay in the onset of recovery after pumping stopped and the shift of the residual

Figure 38: Hydrograph data from M-1 and M-2.

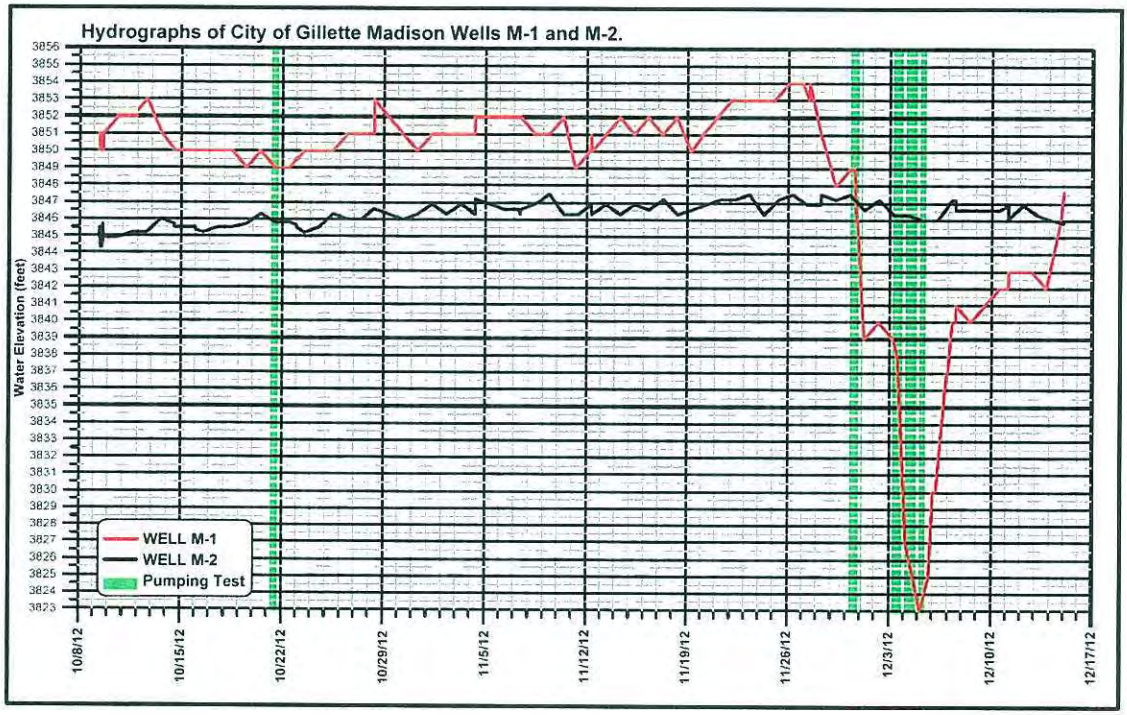

Figure 39: Time-drawdown plot for existing well M-2.

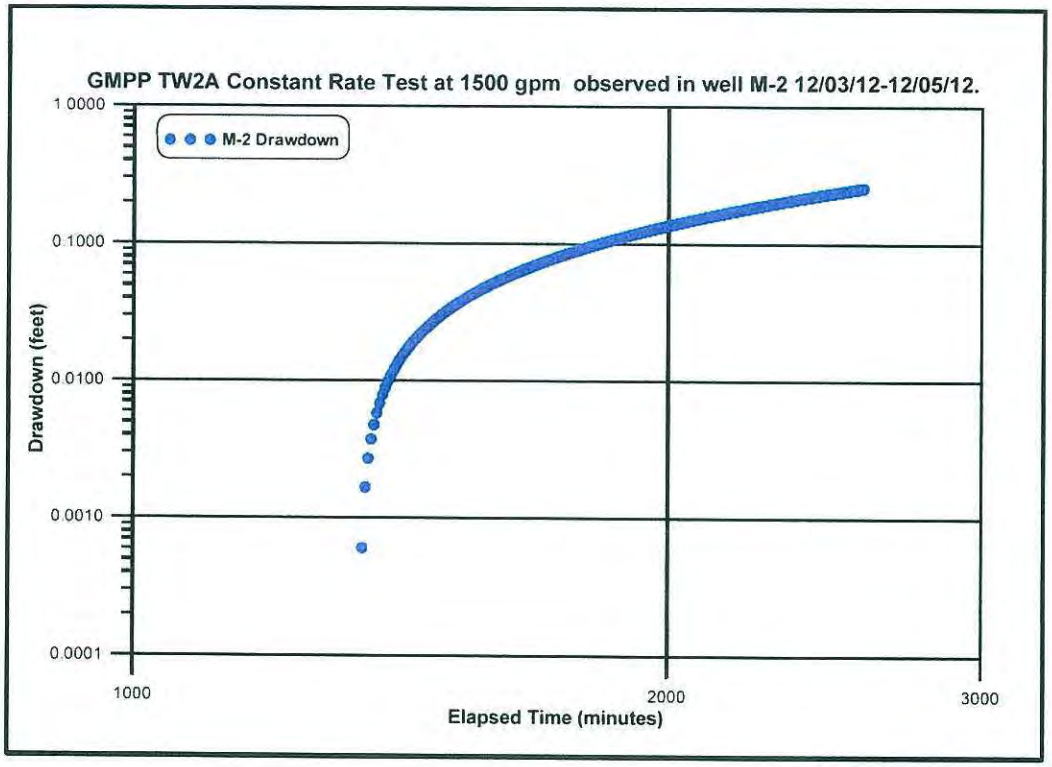

Figure 40: Semilogarithmic time-drawdown plot of M-1 response to 1500 gpm at TW#2A.

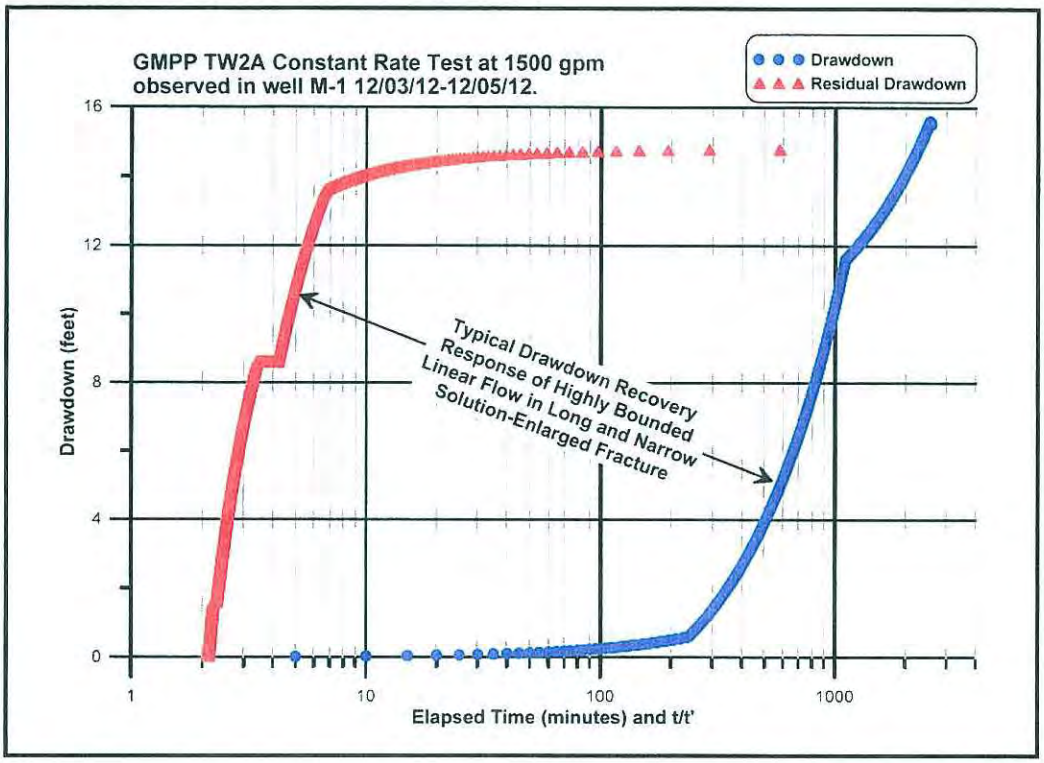

drawdown curve to the left of the drawdown curve are both diagnostic of linear flow on this type of plot; i.e., the flow at the observation well is along a narrow feature such as a solution-enlarged fracture. This is the type of aquifer response observed at wells M-1, M-2, M-3, M-4 and M-8 through M-10 in the existing City of Gillette Madison wellfield, when they were subjected to pumping tests. A solution-enlarged fracture is consistent with the known geology and geologic history of the Madison aquifer in this region.

Figure 41 shows a diagnostic log-log plot of time-drawdown data observed in existing well M-1 during the 1500-gpm test of TW#2A. The first approximately 140 minutes of drawdown takes place at a log-log unit slope (one log cycle of drawdown for one log cycle of elapsed time). A log-log unit slope at a constant rate of pumping is one in which drawdown is directly proportional to the pumping rate and is typical of the drawdown that occurs in a storage tank pumped at a constant rate or in a well casing where the initial flow of water to the pump is almost all derived from water stored in the casing above the pump.

After the initial log-log unit slope response, the time-drawdown response makes a transition to a rate of drawdown that is essentially a log-log quarter unit slope (one log cycle of drawdown for four log cycles of elapsed time). The small recovery of drawdown

Figure 41: Double logarithmic plot of time-drawdown response in well M-1.

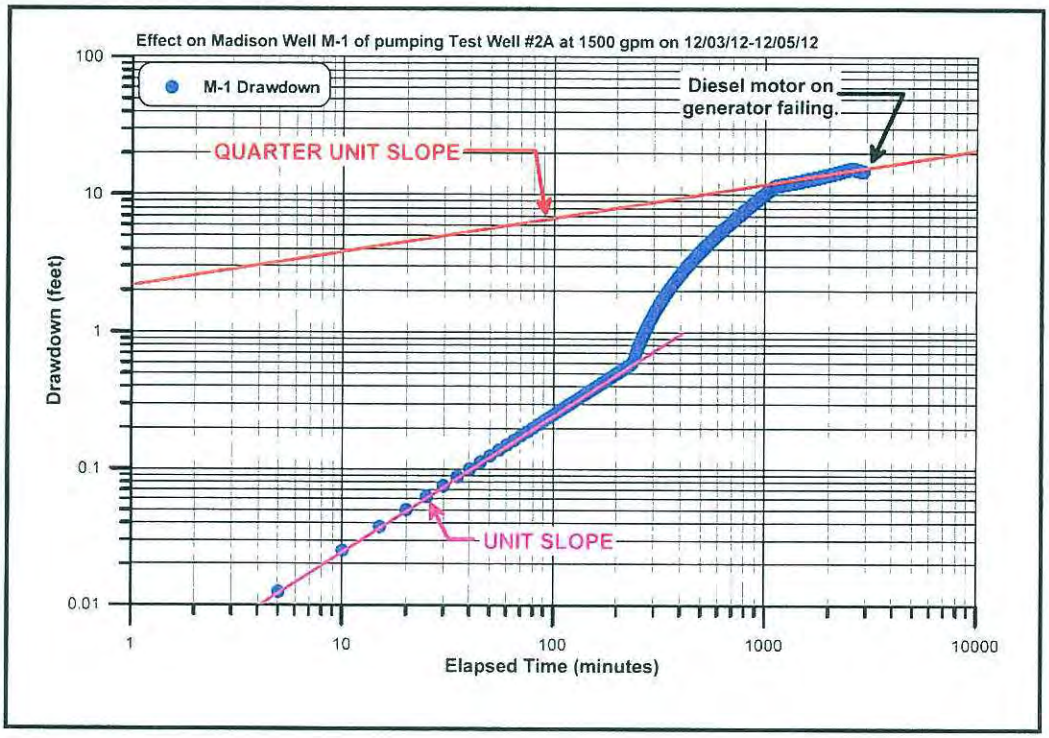

at the end of the test resulted from failure of the diesel motor driving the generator and a consequent decrease in the pumping rate due to a decrease in the power delivered to the VFD on the test pump.

All linear flow time-drawdown response on log-log plots is a straight line. The straight line will exhibit different slopes for different types of linear flow. The principal difference between different types of linear flow is the source of water released from groundwater storage to supply the water pumped from the well.

The unit slope response is typical of water provided to a pump by casing storage or, in some large fractures, from a large natural void where drawdown is essentially uniform throughout the void. The half unit slope response results from release of water from storage in the fracture, with a hydraulic gradient along the fracture to the pumped well. Quarter unit slope response indicates the fracture has become a conveyance system and is no longer releasing groundwater from storage. The water conveyed through the fracture under quarter unit slope conditions is released to the fracture from groundwater storage in the rock surrounding the fracture and, in the mathematical theory, is flowing perpendicular to the fracture as it is released from storage. As the latter type of flow expands the area depressurized or dewatered around the fracture, a large ellipsoidal area of drawdown analogous to a cone of depression develops and as the flow into the fracture becomes less perpendicular to the fracture walls, pseudo-radial flow develops in which the portion of the fracture conveying water to the pumped well acts as an elongate, large-diameter well.

The theoretical succession is unit slope to half unit slope to quarter unit slope. Quarter unit slope may become less than a quarter unit slope straight line if recharge is provided by cross-cutting fractures. Otherwise; quarter unit slope response transitions into pseudo-radial flow at long pumping times. Typically, fracture geometry, hydraulic properties and interaction with porous host rock prevent pumped fractures from showing all of the above phases of linear flow or they each persist for such a short time that they cannot be distinguished from the transition from one to another. This is often most evident in time-drawdown curves that go directly into quarter unit slope flow shortly after pumping starts. Another typical response is a half unit slope response that persists until the drawdown in the pumped well causes the well yield to decline. This latter response is that of a fracture full of water and surrounded by essentially impervious rock and not connected to other fractures.

The foregoing principles of linear flow interpretation are the basis for interpretation of the aquifer response observed at existing City of Gillette Madison well M-1 when well TW#2A was tested for two days at 1500 gpm. As discussed above and shown in Figures 35 and 36, aquifer response at pumped well TW#2A was that of radial flow. Accordingly, a so-called "cone of depression" was spreading out from TW#2A in which the pressure in the confined aquifer was being reduced along a gradient back to the pumped well, as reflected by the time-drawdown response. Also known from previous studies of the existing City of Gillette Madison Wellfield is that all of the wells, with the exceptions of Wells M-5, M-6 and M-7; are in direct hydraulic communication with a large solution-enlarged fracture in the Madison aquifer and they exhibit diagnostic linear flow response during pumping tests.

Well M-1 is near the northern end of the recognized extent of a topographic lineament interpreted to be the trace of the large fracture penetrated by seven of the wells in the existing wellfield. The outward expanding cone of depression around pumped well TW#2A began to depressurize the confined Madison aquifer containing the large fracture at M-1 nearly immediately, as shown by the time-drawdown plot on Figure 41, where a drawdown of less than 0.02 feet was recorded five minutes after the pumping test began. The data from well M-1 was collected by the City of Gillette SCADA system at a 5-minute frequency starting at the beginning of an hour.

As the host rock containing the fracture was depressurized, the fracture began to release groundwater storage into the porous host rock. Water provided from storage in the fracture supports part of the pumping rate, so the rate of groundwater release from the porous rock around the pumped well can decrease, as shown by the "recharge" effect on Figure 35.

For the first 140 minutes of release of groundwater storage from the fracture, drawdown at M-1 was less than 0.6 feet. This was not enough drawdown at the northern end of the fracture to initiate a significant hydraulic gradient or flow of water along the fracture toward the cone of depressurization. As drawdown in the fracture exceeded about 0.6 feet, a flow of groundwater was initiated along the fracture with an associated

release of groundwater storage taking place in the fracture, and the rate of drawdown in the fracture departed from the unit slope response.

After departing from the unit slope response, the release of groundwater storage from the fracture into the radial flow cone of depressurization resulted in a time-drawdown response transitioning toward a log-log half unit slope. The rate of drawdown for the log-log plot in this period of transition was undoubtedly accelerated by the rate of radial flow drawdown in the host rock surrounding the fracture.

After approximately 1000 minutes and 10 feet of drawdown, the time-drawdown curve in the fracture, as observed in well M-1, entered a quarter unit slope response (Figure 41). A quarter unit slope response indicates the rate of drawdown in the fracture is controlled by the rate of release of groundwater from storage in the porous rock containing the fracture. In this case, the radial cone of depression from the pumped well is lowering the pore pressure in the porous rock surrounding the fracture at the old wellfield, so release of that same storage into the fracture to control the rate of drawdown is circular reasoning. Therefore, it is necessary to seek an alternative explanation for the quarter unit slope rate of drawdown in the late part of this test.

An alternate explanation is that the solution enlarged fracture penetrated by well M-1 and other wells in the existing COG Madison Wellfield is not the fracture that is influencing the rate of drawdown observed in well M-1. The rate of drawdown may be controlled by some other fracture near the pumped well. A potential candidate for this role would be a solution enlarged fracture aligned west-northwest to east-southeast along the large coulee located approximately 1800 feet north of TW#2A. This hypothetical fracture is about 1000 feet closer to pumped well TW#2A than the northern end of the fracture penetrated by well M-1, and would therefore begin to influence the rate of drawdown in the affected area well before the fracture penetrated by well M-1. Likewise, the orientation of the hypothetical fracture would allow it to exhibit a quarter unit slope response while affected by radial flow drawdown impinging on it from the pumped well to the south. Based on these considerations, it is concluded that the observation well response observed at well M-1 may be influenced not only by the presence of the COG Madison Wellfield fracture, in the early unit slope response, but by another fracture nearer to the pumped well in later quarter unit slope response, potentially a solution enlarged fracture aligned with the major coulee north of the pumped well.

As the radial flow cone of depression impinged on the hypothetical fracture to the north, a hydraulic gradient developed along that fracture until groundwater was released into the fracture from the surrounding bedrock. The water released in storage from the surrounding bedrock was then conveyed along the fracture to where it flowed from the fracture and into the radial cone of depression where it intercepted the fracture. The release of groundwater storage into the fracture from the surrounding rock took place along the north side of the fracture and along those parts of the south side of the fracture not affected by the radial flow cone of depression. The fact that the radial flow cone of depression prevented some release of groundwater storage into the

hypothetical fracture from the surrounding porous rock is reflected in the fact that the late test response shown on Figure 41 is slightly steeper than a quarter unit response.

The quarter unit slope response and modified quarter unit slope in the late part of the aquifer test, as shown on Figure 41, is the result of linear flow drawdown in an unidentified fracture, hypothetically located north of the pumped well, controlling the rate of drawdown. Therefore, the difference in quarter-unit slope drawdown and the observed drawdown is equal to the component of radial flow drawdown in the aquifer at the observation well. Figure 42 shows the total observed drawdown, the unit slope drawdown and the radial flow drawdown on a semilogarithmic plot. The radial flow drawdown added to the quarter unit slope drawdown equals the total drawdown.

Figure 42: Separation of late drawdown into linear and radial flow components.

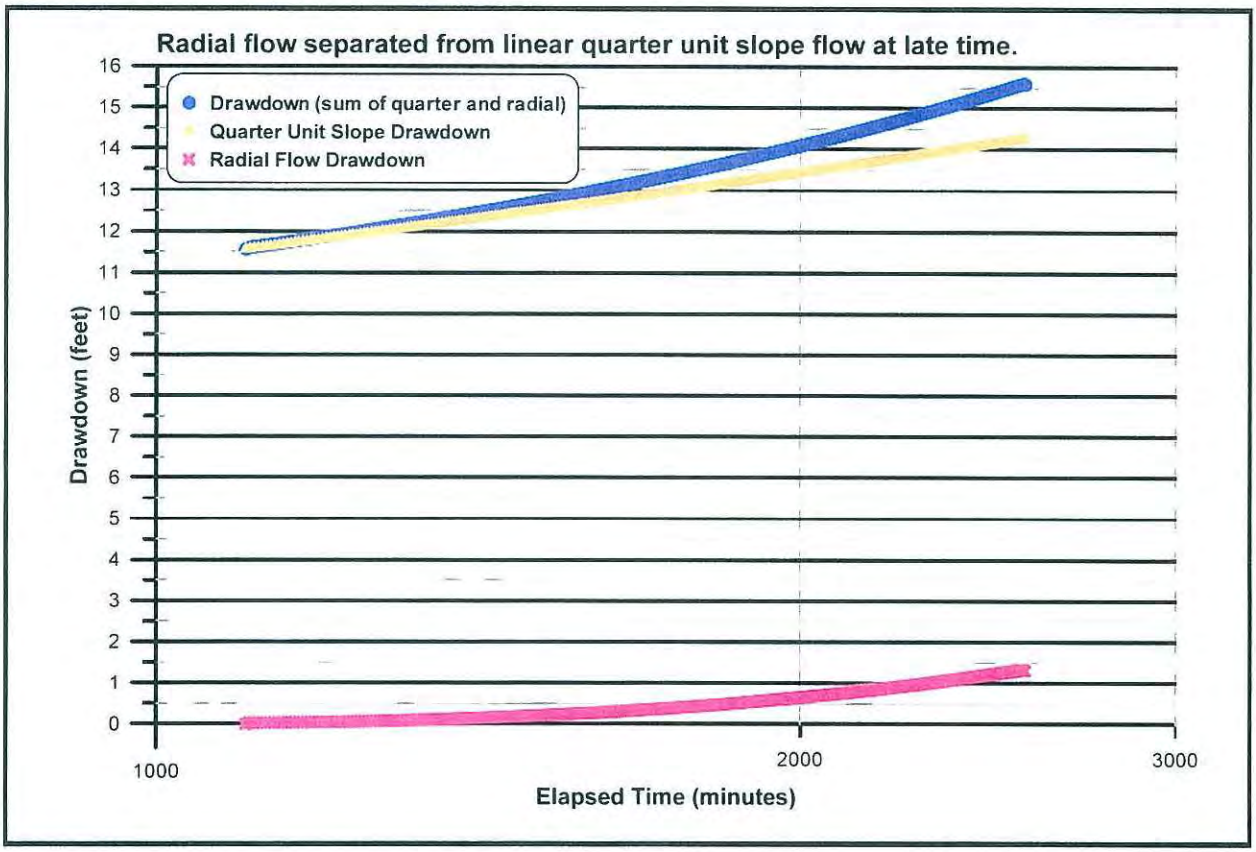

The measureable expansion of the radial flow component of drawdown at the location of well M-1 should conform to the Theis non-equilibrium for radial flow. If it does conform to the Theis type curve, it can be projected with the type curve. Figure 43 shows a semi-logarithmic form of the type curve fit to the radial flow drawdown component. The radial flow drawdown and the quarter-unit slope drawdown are projected to 70 days, (100,800 minutes), providing drawdowns of approximately 29 feet and 36 feet, respectively, for radial and linear flow drawdown.

Figure 43: Projection of drawdown at M-1 to 70 days of pumping Test Well 2A at 1500 gpm.

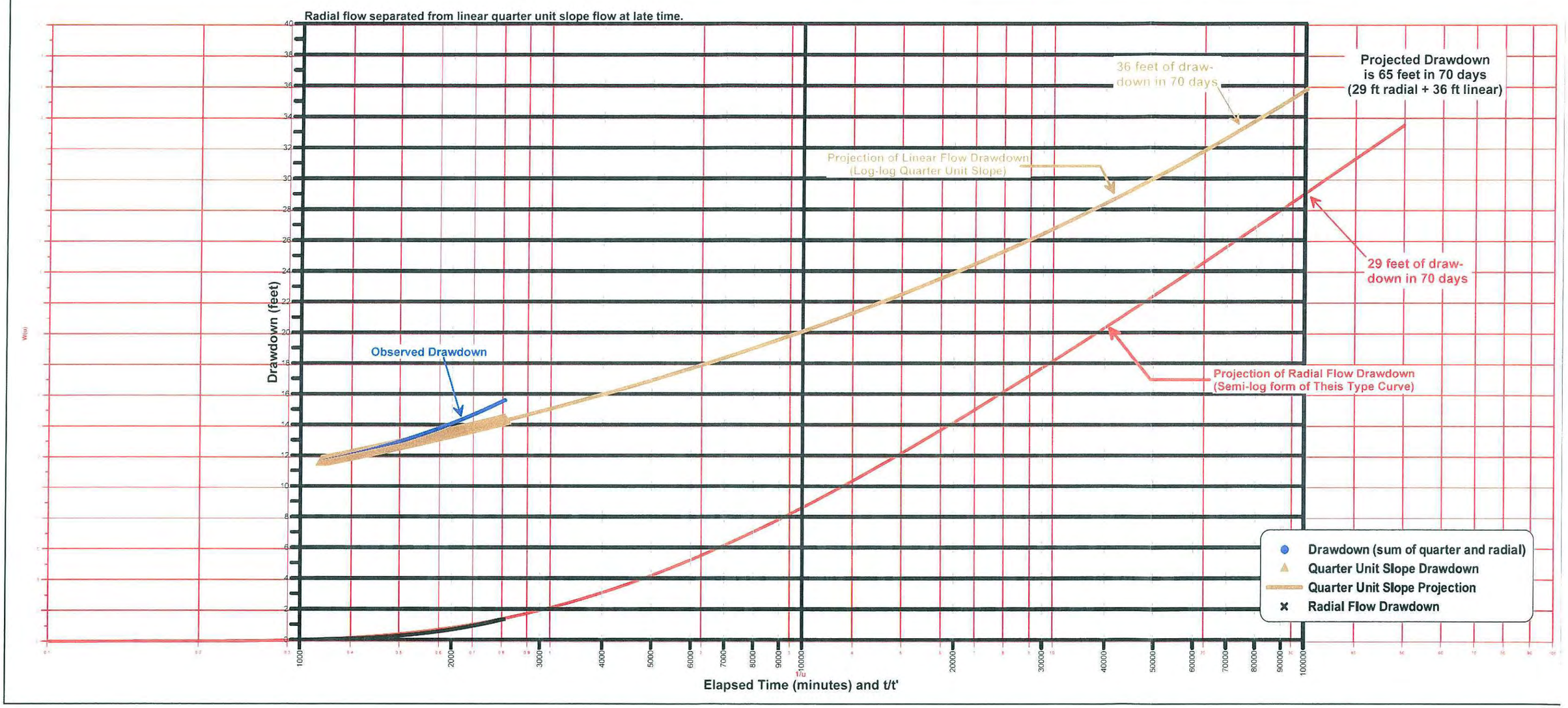

Based on the projections of drawdown shown on Figure 43, total drawdown at well M-1 at the end of 70 days of pumping a constant 1500 gpm from Test Well 2A is 65 feet; i.e., the sum of 29 and 36 feet of drawdown. The reported depth to the pump is 895 feet and the static water level in October through December 2012 fluctuated around 460 feet below ground level, providing approximately 435 feet of water over the pump at that time. City of Gillette staff report the minimum non-pumping water column height over the pump in 2012 was 361 feet. An additional 65 feet of drawdown at well M-1, due to operation of Test Well #2A, might diminish the output from the pump in well M-1, but would not diminish the well yield available from the well.

For the sake of comparison of this information with Figure 38, the approximate elevation of well M-1 is 4309 feet and the pump inlet elevation in well M-1 is approximately 3414 feet. Figure 38 shows that the water surface elevation at M-1 was about 3850 feet during the aquifer test; providing more than 430 feet of water column over the pump. The water column over the pump with the pump operating should be verified, but if it is in the order of 360 feet, an additional 65 feet of drawdown from Test Well 2A will not diminish the well yield of well M-1, even if the discharge rate provided by the existing production pump is diminished by the additional discharge head.

Figure 44 shows historic static and pumping water levels for well M-1 from 1981 through the end of 2006, as well as a partial record of pumping rates for that period of time. Figure 44 shows a general static water level depth of 500 feet or slightly less in the 26-

Figure 44: Static and pumping water levels for Well M-1 through November 2006.

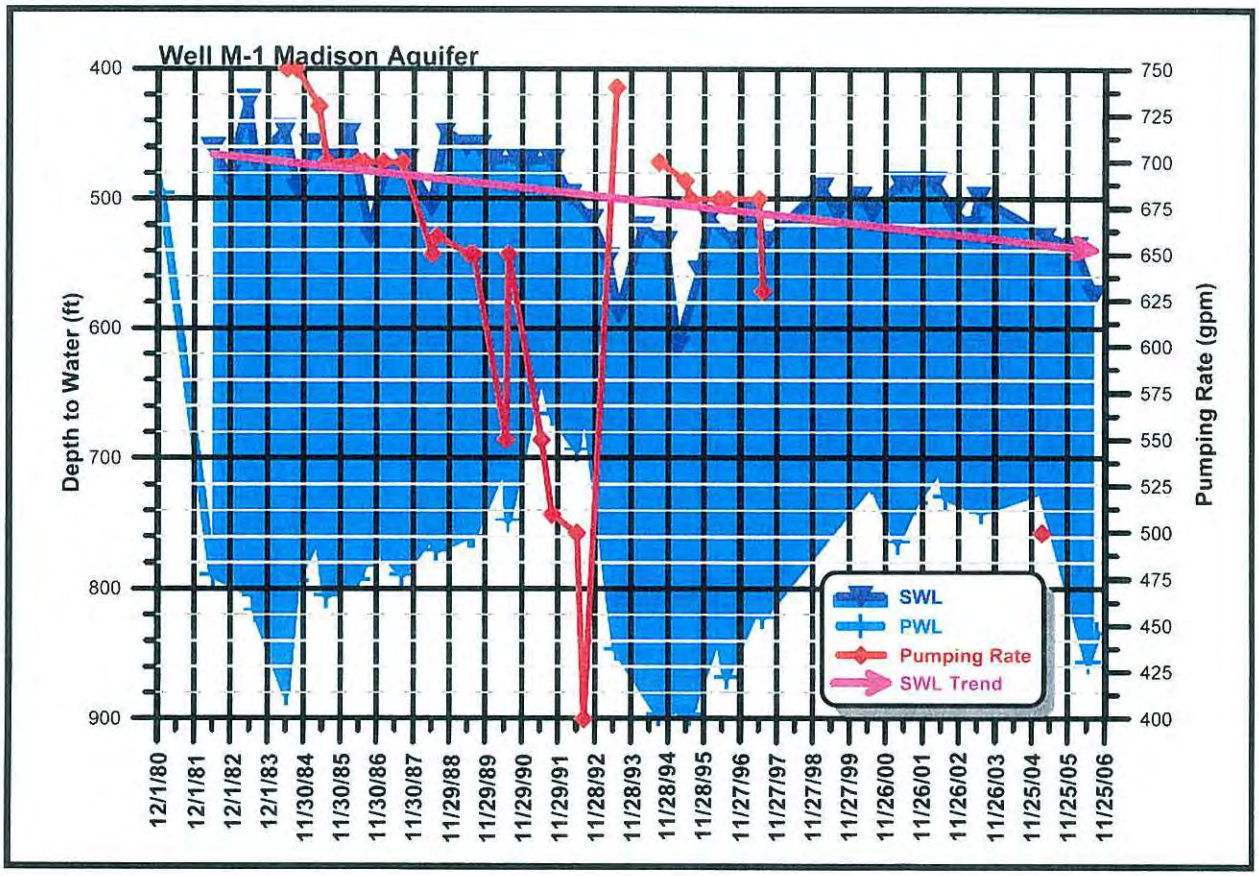

year record, or a typical pump submergence of approximately 440 feet from 1981 through 1990 and about 400 feet from 1998 through 2002. Less than 400 feet of pump submergence was available in other times during the period of record, when high pumping rates were in effect, presumably with associated long pumping duration.

For example, Figure 45 indicates that when pumping rates were 750 gpm in 1983, the pumping water level was nearly at the current pump inlet depth of 895 feet. Reducing the pumping rate to 700 gpm in 1984 through 1987 provided about 100 feet or more of pump inlet submergence, assuming the pump inlet was at 895 feet. Static water levels declined somewhat during the same period of time ending in 1987. Static water levels recovered and remained slightly above 470 feet from 1988 through 1990, even as the pumping rate declined, evidently due to deteriorating pumping equipment. Even so, the static water level records reflect a decline in 1991, with the lowest pumping rates on record, probably because the pump was not off long enough for a true static water level to be recorded. Evidently a new pump was installed in late 1991, causing the pumping rate to increase to about 730 gpm or more, and the pumping water level to decline by 200 feet in 1992 and 1993, lowering the pumping water level to essentially the currently reported pump inlet depth of 895 feet. A reduction in the pumping rate to about 680 gpm in late 1993 was followed by recovery of the pumping water levels by about 50 feet and a slow recovery of the static water level.

Based on Figure 45 pumping and water level records, it is clear that the impact of pumping Test Well #2A on well M-1 will depend on the pumping rate and duration at well M1. If the pumping rate at M-1 is maintained at 650 gpm or less, the drawdown interference from production pumping at Test Well #2A will have little effect on the pumping rate from well M-1. Short periods of pumping at Test Well #2A up to 680 gpm might be tolerated for short times, but should be avoided. The historic record on Figure 45 indicates that when pumping rates of 700 gpm or more are maintained at M-1, the pumping water level becomes too low, declining to the pump inlet depth at 895 feet, and any interference drawdown from Test Well #2A will diminish the potential yield at M-1.

5.4.3 Aquifer Hydraulic Parameters

Figure 45 shows the total observed drawdown, the quarter unit slope drawdown and the radial flow drawdown observed at well M-1 with the Theis type curve visually fit to the radial flow component of the drawdown. A match point for the Theis solution is shown and the calculations for the Theis solution are shown.

The Theis solution provides an aquifer transmissivity value of T = 460 ft^2/day and an aquifer storage coefficient (storativity) value of S = 0.0012. The transmissivity value of 460 ft^2/day compares favorably with the value of 446 ft^2/day determined by the Cooper-Jacob solution applied to the data at the pumped well.

The fit of the Cooper-Jacob solution to the pumped well data is recognizably better than the fit of the Theis type curve to the mathematically derived radial flow data for well M-1 and is likely the better representation of the aquifer transmissivity. However, the aquifer storativity, S, cannot be calculated from a single well test and the calculation is dependent on the value of aquifer transmissity at an observation well. Therefore, the

aquifer storativity value of 1.2×10^{-3} is dependent on the transmissivity value determined at well M-1.

Both of the transmissivity values substituted into the storativity calculation provide the same result when rounded to 10^{-3}. This, plus the fact that the transmissivity value derived by separating drawdown components at well M-1 is in good agreement with that derived from the pumped well data, lends support to the conclusion that the aquifer storativity is genuinely in the order of 10^{-3} and that reinterpretation of the data with aquifer test software is unlikely to change that conclusion. Aquifer test software is not designed to make the separation between linear flow drawdown and radial flow drawdown that must be made before the aquifer test response at well M-1 can be interpreted. Therefore, any application of aquifer test software to interpret the M-1 time-drawdown response without pre-processing the data as shown herein will yield erroneous and misleading results.

It should also be noted from Figure 45 that projection of drawdown at well M-1 based on the Theis type curve appears to overestimate drawdown when compared to the radial flow curve separated out of the total observed drawdown. Therefore, the projection of radial flow drawdown shown on Figure 43, is conservatively large.

6 WATER QUALITY

A water quality sample taken from the discharge water during air rotary drilling provided a total dissolved solids (TDS) value of 676 mg/L for water from the Madison aquifer. Subsequent chemical analyses of the aquifer water quality from Test Well #2A are of samples collected after treatment of the aquifer with concentrated acid to stimulate aquifer production to the well. Monitoring of the electrical conductance of the water pumped from the aquifer during the 48-hour yield and drawdown test of the well, as shown on Figure 19, recorded initially high TDS concentrations that steadily decreased to a final TDS concentration of 891 mg/L at the end of the test. As shown by the pre-acid treatment sample collected from the air lift discharge, the final TDS value of 891 mg/L reflects the remaining influence of the acid treatment on water quality.

The test pump generator failed two minutes short of 48 hours of constant rate testing. A water quality sample was not obtained during this constant rate test, which ended 12/5/2012, because failure of the generator was not anticipated. Accordingly, a sample of the water was collected for laboratory analysis on 12/13/2012. This was accomplished with a 175 to 200 gpm pumping rate, using a small pump temporarily installed into the well for final disinfection after the large test pump had been removed.

Continued pumping of the well, combined with increased time for natural diffusion and dilution of the water in the aquifer near the well, will ultimately result in the water quality returning to pre-acid treatment conditions. The water quality laboratory analytical reports are shown in Appendix F. One report shows the total dissolved solids concentration after acid treatment of the well. The other report is for the sample taken on 12/13/2012, eight days after the constant rate test inadvertently ended.